ELSEVIER

Contents lists available at ScienceDirect

Forest Ecology and Management

journal homepage: www.elsevier.com/locate/foreco





Biophysical drivers of short-term change in evapotranspiration after fire as estimated through the SSEBop Landsat-based model

José Manuel Fernández-Guisuraga ^{a,b}, Carmen Quintano ^{c,d,f,*}, Alfonso Fernández-Manso ^{e,f}, Dar A. Roberts ^f

- a Department of Biodiversity and Environmental Management, Faculty of Biological and Environmental Sciences, University of León, León 24071, Spain
- b Centro de Investigação e de Tecnologias Agroambientais e Biológicas, Universidade de Trás-os-Montes e Alto Douro, Vila Real 5000-801, Portugal
- ^c Electronic Technology Department, School of Industrial Engineering, University of Valladolid, Valladolid 47011, Spain
- ^d Sustainable Forest Management Research Institute, University of Valladolid, Palencia 34004, Spain
- e Agrarian Science and Engineering Department, University of León, Av. Astorga s/n, Ponferrada 24400, Spain
- f Department of Geography, University of California, Santa Barbara, CA 93106, USA

ARTICLE INFO

Keywords: Fire severity Evapotranspiration Mediterranean countries FCOVER

ABSTRACT

Wildfires in Mediterranean countries are increasingly frequent, extensive, and ecologically damaging, impacting not only vegetation and soil but also the water cycle, specifically altering evapotranspiration (ET). Following a wildfire, ET values experience a sharp decline, which persists until vegetation returns to its pre-fire state. This study examines the factors influencing this reduction, focusing on fire severity, topography, ecosystem type (broadleaf, conifer, mixed forests, and shrublands), and pre-fire fuel conditions, including fractional vegetation cover (FCOVER) from PROSAIL-D RTM inversion of Landsat 8 OLI images and structural complexity from Sentinel-1 SAR, on ET 1-year after fire. Given the heterogeneous nature of Mediterranean landscapes, where vegetation and water availability vary widely, fine spatial resolution ET models are essential. This study utilized the Operational Simplified Surface Energy Balance (SSEBop) model to estimate ET from Landsat imagery, focusing on four major wildfires that occurred in Spain and Portugal in 2022. Random Forest regression identified fire severity and pre-fire FCOVER as the most influential factors in ET reduction. Results showed that fire severity's impact on ET reduction followed a consistent pattern across ecosystems, with the greatest relative reductions observed in shrublands, followed by conifer and broadleaf forests. The most pronounced reductions occurred in areas of higher fire severity. In conclusion, fire severity emerges as a key driver of short-term changes in ET in Mediterranean environments. This study underscores the value of Landsat-based ET models as reliable tools for assessing the ecological consequences of fire severity in these regions.

1. Introduction

As a recurring natural disturbance across the Mediterranean land-scape, wildfires are increasing both in frequency and extent (Jones and Tingley, 2022; Koutsias et al., 2022; Seidl et al., 2014). In the Mediterranean Basin, the combination of more frequent hot, dry summers, and fuel buildup over time and space has been shown to lead to longer, more severe fire seasons (Fernandes, 2013), which has wide-ranging environmental, economic and social impacts (Beltrán-Marcos et al., 2024; Turiel-Santos et al., 2024). Increasing fire incidence affects not only vegetation and soil, but also water balance cycle, including evapotranspiration (ET) (Clark et al., 2012; Li et al., 2018). ET refers to the

process through which water is conducted to the atmosphere from the earth's surface by both evaporation from soil and other surfaces, and by transpiration from plants (Thornthwaite, 1948). It is a crucial component of the hydrological cycle, influencing water availability and modulating local and regional climate through its effects on surface energy balance, humidity, and atmospheric circulation (Allen et al., 1998). Its decline after a wildfire because of a loss of LAI or transpirational surface area due to vegetation consumption during the fire event (Mankin and Patel, 2021) can alter local and regional weather patterns, soil moisture dynamics and vegetation recovery (Bond-Lamberty et al., 2009; Ueyama et al., 2014). The ET rate depends on several factors, including solar radiation, wind speed, humidity, temperature, and the

^{*} Corresponding author at: Electronic Technology Department, School of Industrial Engineering, University of Valladolid, Valladolid 47011, Spain. E-mail address: carmen.quintano@uva.es (C. Quintano).

type and density of vegetation (Yao et al., 2013). Soil moisture and land use (e.g., agricultural fields, forests) significantly impact ET rates; forests generally have higher ET due to their larger leaf area compared to other land types (Liang et al., 2024). Thus, ET demonstrates significant heterogeneity across the land surface, driven by intricate environmental controls and biophysical feedback mechanisms. (Yuan et al., 2010).

Following a wildfire, ET values decrease sharply because of reduced leaf area, disturbing the water balance of the affected area (Fernández-Manso et al., 2020; Mankin and Patel, 2021). This reduction in ET is not a short-term phenomenon, but can persists for several years to even decades until the vegetation fully recovers, depending on the characteristics of the ecosystem and fire severity (Ma et al., 2020; Collar et al., 2023; Ahmad et al., 2024; Norlen et al., 2024). Numerous previous studies investigating the connection between fire impacts and ET have utilized field-measured surface fluxes (Bond-Lamberty et al., 2009; Nolan et al., 2015; Dore et al., 2010; Clark et al., 2012; Ueyama et al., 2014), due to the difficulties in accurately estimating ET at a suitable spatial resolution using satellite data (Van der Tol and Norberto-Parodi, 2011; Yi et al., 2024). Fine spatial resolution satellite data that estimate ET accurately have become recently available (Baris and Tombul, 2024), however these data products enhance our ability to assess long-term patterns and comparing data across various regions or wildfire events (Quintano et al., 2024). Most remote sensing-based ET models depend on either full or simplified versions of the energy balance equation (Baris and Tombul, 2024; de la Fuente-Sáiz et al., 2017). This equation accounts for the energy used to convert liquid water in soil and plants into water vapor, which is then released into the atmosphere (Zhang et al., 2016). Among the models based on the full version of the energy balance equation are: the Surface Energy Balance Algorithm for Land (geeSE-BAL) (Laipelt, et al., 2021), the Google Earth Engine (GEE) implementations of Mapping Evapotranspiration at High Resolution with Internalized Calibration (eeMETRIC) (Allen et al., 2007, Allen et al., 2018), and the Atmosphere-Land Exchange Inverse/Disaggregation of the Atmosphere-Land Exchange Inverse (ALEXI/DisALEXI) (Anderson et al., 2007, Anderson et al., 2018). Simplified methods that either omit certain parameters of the energy balance equation or use simplified assumptions include the Priestley-Taylor Jet Propulsion Laboratory (PT-JPL) (Fisher et al., 2008), and the Operational Simplified Surface Energy Balance (SSEBop) (Senay et al., 2013, 2022, 2023; Senay, 2018). Particularly, the United States Geological Service's (USGS) 30-m operational SSEBop product provides adequate accuracy, ease of downloading, less complex implementation and lower associated costs than other ET models (Filippelli et al., 2022; Quintano et al., 2024; Zimba et al., 2024). However, to our knowledge, only Mankin and Patel (2021); (2023) and Quintano et al. (2024) have related the 30-m SSEBop ET Landsat-based product to fire related processes. The 70-m ECOSTRESS-based ET product, although slightly coarser in resolution than the 30-m Landsat-based SSEBop ET product, has also been successfully used in wildfire-related studies at local to regional scales (e.g., Poulos et al., 2021; Pascolini-Campbell et al., 2022; Wilder and Kinoshita, 2022; Joshi et al., 2024). In contrast, the 1-km MODIS-based ET product is typically applied in regional to global scale analyses (Shrestha et al., 2022; Nguyen et al., 2025).

Multiple elements influence the extent of post-fire reduction in ET. Fire severity, understood as the degree of vegetation mortality caused by the fire event (Keely, 2009), plays a crucial role (Mankin and Patel, 2023; Han et al., 2024). More severe fires tend to destroy a larger portion of the plant biomass, significantly diminishing ecosystem evapotranspiration (Poulos et al., 2021). Fire severity is usually estimated by using remote sensing data and techniques, as the exclusive use of field measurements is costly in time and resources, especially in extensive burned areas (Key and Benson, 2006). Fire severity is typically assessed by observing post-fire vegetation changes in spectral indexes base on red, near-infrared (NIR), and/or short-wave infrared (SWIR) spectral bands of multispectral data (e.g. Quintano et al., 2018; García-Llamas et al., 2019a; Fernández-Guisuraga et al., 2024a). In

particular, the differenced Normalized Burn Ratio (dNBR, Key and Benson, 2006), calculated from NIR and SWIR bands, is a widely-used metric(e.g. Boucher et al., 2017; Fernández-Manso et al., 2019; Chen, et al., 2021; Fernández-Guisuraga et al., 2024b), made available through Monitoring Trends in Burn Severity (MTBS) in the United States (Eidenshink et al., 2007), and the European Forest Fire Information System (EFFIS) through its Rapid Damage Assessment module.

Topographic factors like altitude and terrain slope also influence post-fire reduction in evapotranspiration (ET) values. These variables can alter local microclimates, affecting factors such as wind patterns, soil moisture availability, and temperature (Ireland and Petropoulos, 2015; Zahura et al., 2024). As a result, topographic factors can slow down or accelerate the recovery of vegetation (Lippok et al., 2013; Petropoulos et al., 2014), directly impacting ET rates. Elevation can also either positively or negatively affect vegetation recovery by influencing precipitation patterns and local temperature values (Meng et al., 2015; Viana-Soto et al., 2020); slope can also have an effect on the vegetation recovery by impacting soil erosion and water retention (Christopoulou et al., 2019; Evangelides and Nobajas, 2020), as can aspect by affecting insolation (Ireland and Petropoulos, 2015; Rengers et al., 2020). Besides fire severity and topographic factors, pre-fire vegetation conditions can offer valuable predictions about how a given area may respond to wildfires (Martinson and Omi, 2013; Fernández-Guisuraga and Calvo, 2023) and how ET might be altered by fire (White et al., 2020; Collar et al., 2023). In general, vegetation types show different responses to fire and the consequent impacts on ET (Zhao et al., 2016; Zhu et al., 2024). Broadleaf forests, conifer forests, mixed forests, and shrublands show substantial differences in their ability to retain water (Stephenson, 2003; Mészároš and Miklánek, 2009) and recover after a fire (Roche et al., 2020). Following a fire, conifer forests typically suffer greater reductions in ET due to the high flammability of their components, which is linked to their composition and structure. In contrast, shrublands, with their lower biomass and higher adaptability to frequent fires, tend to exhibit faster recovery (Roche et al., 2020), and higher post-fire ET (Poulos et al., 2021).

Understanding the drivers of ET reduction after wildfires is essential for establishing effective fire management policies and predicting the recovery trajectory of affected ecosystems (Ma et al., 2020). Previous studies have proven that ET is highly influenced by various environmental factors such as fire severity, vegetation cover, and topographic characteristics (Collar et al., 2023; Mankin and Patel, 2023; Zahura et al., 2024). However, the specific mechanisms through which these factors interact and contribute to the post-fire decline in ET remain poorly understood, particularly in Mediterranean landscapes where ecosystem heterogeneity is pronounced. In this study, we investigate the short-term effects of wildfires on ET in four large fire-affected areas in Spain and Portugal during 2022. Using high-resolution remote sensing data and the Operational Simplified Surface Energy Balance (SSEBop) model, we assess the role of fire severity, pre-fire vegetation and topography in determining ET reduction 1-year after the fire. The first year is particularly important, as it typically sets the foundational trends in post-fire water balance dynamics, though it represents a relatively short time frame for meaningful vegetation recovery. By integrating multiple data sources, including Landsat 8 OLI and Sentinel-1 SAR imagery, we aim to provide a comprehensive analysis of the key drivers behind ET dynamics in Mediterranean wildfires. Thus, the main novelties of this study are related to the methodology, as it provides a different and simpler approach than full water balance models. First, the study is based on operational fine spatial resolution ET products. The use of fine spatial scale to understand water balance dynamics associated with fires let to link vegetation responses to environmental variation. The spatial resolution of this approach contrasts with previous studies using low spatial resolution -1 km-, which is appropriate to regional but not wildfire-scale analysis (Collar et al., 2023). It also differs from earlier research that relied on empirical ET estimates, such as those derived from NDVI and flux towers (Ma et al., 2020). And second, the study

incorporates pre-fire FCOVER and SAR data (proxy for vegetation structural complexity) as biophysical drivers to predict fire-induced changes in ET behavior. By integrating this information, the analysis accounts for post-fire variations in canopy structure and vegetation density, which are critical for accurately modeling ET dynamics (Shaver, (2011)). Consequently, this research emphasizes the importance of fine-scale ET modeling for improving our understanding of ecosystem responses to fire, while also contributes to the literature on wildfire impacts in Mediterranean regions. In addition, the findings of this study will offer valuable insights for post-fire management and restoration strategies in the context of climate change, which is presumed to

exacerbate wildfire intensity and frequency in the Mediterranean Basin (Aparício et al., 2022).

2. Material

2.1. Study sites

Four wildfires (Fig. 1) located in northwestern Spain were selected for analysis. The sites cover a broad spectrum of topographic conditions, with different elevation and slope ranges (Table 1), although none of the sites has a complex topography, which is significant for the accuracy of

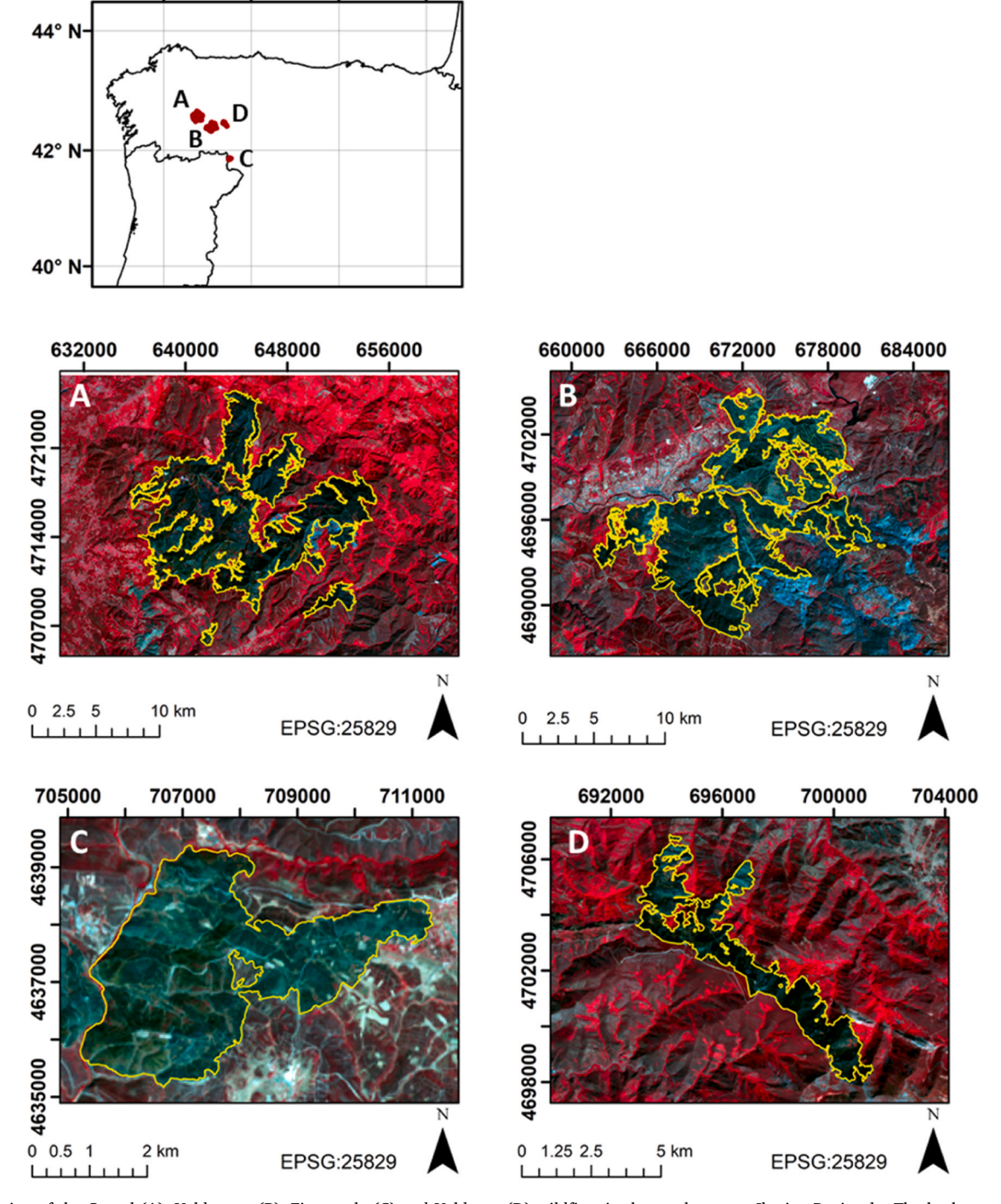


Fig. 1. Location of the Courel (A), Valdeorras (B), Figueruela (C) and Valdueza (D) wildfires in the northwestern Iberian Peninsula. The background image is a Landsat-8 false color composite ($R = 0.85-0.88 \ \mu m$ -band 5-; $G = 0.64-0.67 \ \mu m$ -band 4-; $B = 0.53-0.59 \ \mu m$ -band 3-).

Table 1Environmental characteristics of the four wildfires considered in this study. We incude the number of fire severity reference plots established within each ecosystem type and the image dates of SPOT6/7 post-fire scenes used to estimate fire severity through visual inspection.

Environmental characteristics							
Study site	Wildfire		Topography		Climate		
	Size (km²)	Alarm date	Elevation (m)	Slope (%)	P _{ma} (mm)	T _{ma} (°C)	
Courel	136.12	07/14/2022	500-1350	20-150	1697	10.1	
Valdeorras	127.35	07/15/2022	508-1525	10-130	998	8.8	
Figueruela	11.86	07/15/2022	700-930	0-151	807	11.2	
Valdueza	15.00	07/17/2022	950-1600	0-152	821	10.2	
Fire severity ref	erence plots						
Study site	# Fire severity reference plots					Post-fire SPOT6/7 image date	
	Broadleaf forest	Conifer forest	Mixed forest	Shrubland	Total		
Courel	18	52	12	19	101	07/21/2022 and 07/24/2022	
Valdeorras	10	4	7	26	47	07/21/2022 and 07/28/2022	
Figueruela	9	16	-	17	42	07/27/2022	
Valdueza	8	16	7	19	50	07/23/2022	
Total	45	88	26	81			

the SSEBop ET product. The four study sites have a Csb -Temperate-Mediterranean climate (dry summer)- according to the Köppen-Geiger climate classification, characterized by cold winters and dry and warm summers (AEMET-IM, 2011). The mean annual precipitation and temperature values of each site are shown in Table 1.

This region is among the most wildfire-prone areas in Spain and faces a high risk of experiencing catastrophic events, similar to those that occurred in Portugal in 2017, where over 100 fatalities were reported (Chas-Amil et al., 2020). The selected wildfires occurred during extreme meteorological conditions in summer 2022, characterized by an unprecedented drought and heat waves (Serrano-Notivoli et al., 2023). High temperatures linked to climate change, combined with reduced soil water retention, largely due to cumulative organic carbon losses from recurrent fires (Lombao et al., 2020), have contributed to the emergence of fifth- and sixth-generation wildfires, extreme events that surpass conventional fire suppression capabilities (Regos and Díaz-Raviña, 2023). For instance, the wildfire that occurred in 'O Courel' (Fig. 1, Location A) was classified as a sixth-generation event and was also the largest wildfire ever recorded in the Autonomous Region of Galicia.

The study region has a long-standing history of wildfires (Regos and Díaz-Raviña, 2023), experiencing highly recurrent fire events with short fire-free intervals in some areas. Nearly all wildfires in this region are human-induced; around 82 % are deliberately ignited and classified as arson, while only about 5 % are attributed to accidents or negligence (Chas-Amil et al., 2010). The region is characterized by a mixed-severity wildfire regime. Some areas, such as native broadleaf forests, are typically associated with low-severity fire regimes, whereas others, such as pine-dominated stands, are more frequently affected by high-severity fires

P_{ma}: Mean annual precipitation; T_{ma}: Mean annual temperature.

The information on pre-fire vegetation types for each wildfire was extracted from the Spanish Forest Map at 1:25,000 scale (MITECO, 2019, 2020, 2021). In the four wildfires analyzed (Courel, Valdeorras, Figueruela de Arriba, and Valdueza), the post-fire response of woody vegetation largely depends on the vegetation formation type (forest or shrubland) and the dominant adaptive strategy (resprouting or seeding regeneration) (Pausas and Keely, 2014). In native broadleaf forests, resprouting species capable of regenerating from stumps, rootstocks or epicormic buds dominate, conferring a competitive advantage over seeder species during the early recovery of canopy cover. In contrast, pine plantations mainly rely on seed-based regeneration. For instance, serotinous cones of *Pinus pinaster* open with heat, releasing seeds and promoting high recruitment in the early post-fire stage. Shrublands exhibit two contrasting strategies. Some formations regenerate primarily through persistent soil seed banks that germinate massively after fire. This rapid regeneration often results in communities with high dominance and structurally simple (Parra and Moreno, 2018). In contrast,

other shrubland types are dominated by resprouting species, which also show rapid recovery dynamics (Taulavuori et al., 2013). All these vegetation types are represented across the study sites, enabling comparisons of post-fire impacts on ET among broadleaf forests (Bf), conifer forests (Cf), mixed forests (Mf), and shrublands (S) (Alberdi et al., 2010).

2.2. Background of SSEBop ET model

The SSEBop model estimates ET from satellite imagery, based on a simplified version of the surface energy balance model (Eq. 1) (Senay et al., 2011):

$$R_n = LE - H - G \tag{1}$$

where R_n is the net radiation (W/m^2) , LE is the latent heat flux (W/m^2) , G is the ground heat flux (W/m^2) , and H is the sensible heat flux (w/m^2) .

This model falls under the category of single-source energy balance models, which analyze vegetation and soil as a combined energy budget. These models are particularly convenient for estimating transpiration from vegetated surfaces (McShane et al., 2017). Single source energy balance models estimate sensible heat flux (H) by assuming that the variation in land surface temperature (LST) is linearly related to the temperature difference between the land surface and the air (Su, 2002). This relationship is described by selecting two reference pixels: a "hot pixel," representing bare, dry fields, and a "cold pixel," representing vegetated, wet fields. These two pixels establish a temperature gradient, which is used in an equation to estimate H. These models assumes that the heat flux varies linearly between these two reference points, providing an approximation of surface heat exchange dynamics in the landscape (Senay et al., 2011).

The SSEBop model, unlike other single source energy balance models, does not require the user to select the hot and cold reference pixels for a study area. The SSEBop model uses thermal satellite imagery to estimate land surface temperature (LST, Senay and Kagone, 2019; Hiestand et al., 2024) and calculates de difference between LST and air temperature (Ta) to handle both elevation and latitude effect on surface temperature. This temperature difference is the main driver of the simplified ET calculation as the key assumption in SSEBop is that surface temperature can be used to infer differences in ET between wet (cold) and dry (hot) surfaces. This is possible because the hot and cold reference conditions are predefined for each location and time period through a simplified climatological energy balance approach (Senay et al., 2013). In addition, SSEBop streamlines this process using standardized parameters, making it suitable for large-scale operational use (Singh and Senay, 2016). Detailed information about the SSEBop model can be found in Savoca et al. (2013); Singh et al. (2014); Senay et al. (2022); and FAO, (2023)).

The SSEBop model is a simplified but effective tool for estimating ET.

The model is simpler and more computationally efficient than full energy balance models, making it suitable for real-time applications (McShane et al., 2017). It is scalable; the SSEBop model can be applied at local to global scales using satellite platforms like MODIS, or Landsat, providing ET estimates over large areas (Senay and Kagone, 2019; Hiestand et al., 2024). In summary, it is widely used in water resource management, drought assessment and agricultural monitoring due to its scalability and operational simplicity (e,g. Genanu et al., 2016; Dias Lopes et al., 2019).

2.3. Datasets

The four wildfires occurred in close proximity and almost simultaneously during the summer of 2022 in northwestern Spain. As a result, a single ET scene was sufficient to analyze the four study sites for each selected date. This approach streamlined the analysis and ensured consistent temporal and spatial assessment of ET across the affected areas. We downloaded cloud-free daily ET data with a spatial resolution of 30 m using the SSEBop product (Senay and Kagone, 2019). The selected dates included pre-fire (ET $_{\rm pre}$), immediately post-fire (ET $_{\rm 0-y}$), and multiple dates over the first post-fire year, including 1-year post-fire (ET $_{\rm 1-y}$) (Table 2). These datasets provide a comprehensive temporal sequence to evaluate changes in ET values before and after the wildfires, helping to assess the short-term impacts of fire on the affected ecosystems. This approach ensures high-resolution spatial analysis that aligns with the fine-scale heterogeneity of the Mediterranean landscape.

The official wildfire perimeters were sourced from the Copernicus Emergency Management Service (EMS), and validated by the Spanish regional governments, specifically the Junta de Castilla y León and the Xunta de Galicia. Additionally, SPOT 6 and 7 satellite images, also provided by Copernicus-EMS, were used to gather ground-reference fire severity data at a spatial resolution of 1.5 m (see Table 1).

Additionally, a 25 cm digital elevation model (DEM) from aerial orthophotographs of the Spanish National Orthophoto Program (PNOA) served as the basis for deriving all topographic predictor variables. We used data from the Fourth Spanish National Forest Inventory (SNFI4) and the Spanish Forest Map at a 1:25,000 scale (SFM25) to characterize the ecosystem type; LANDSAT 8 imagery, acquired on the same date as the ETpre, to retrieve FCOVER; and Sentinel-1 data (July 12th, 2022) to obtain the predictors related to pre-fire vegetation structural complexity.

3. Methods

The response of ET to wildfires has been studied from two perspectives: 1) Influence of ecosystem type on the short-term evolution of post-fire ET values; and 2) Impact of environmental factors, such as pre-fire vegetation biophysical conditions and topography, on the reduction of ET 1-year after the fire.

Table 2Acquisition dates of the SSEBop evapotranspiration (ET) product. We also indicate the ET scenario in the pre- and post-fire time series and the Landsat sensor from which the ET estimates have been derived.

Year	Date	Julian day	ET scenario	Sensor
2022	July 8th	189	ETpre	Landsat-8 OLI
	August 9th	221	ET _{0-y}	Landsat-8 OLI
	September 18th	252	-	Landsat-9 OLI2
	October 4th	277	-	Landsat-9 OLI2
	November 5th	309	-	Landsat-9 OLI2
2023	March 21st	80	-	Landsat-8 OLI
	April 6th	96	-	Landsat-8 OLI
	May 8th	128	-	Landsat-8 OLI
	June 25th	176	-	Landsat-8 OLI
	July 19th	200	ET_{1-v}	Landsat-9 OLI2

3.1. ET evolution in the short-term after fire

A regular grid of points with 100-m spacing was used to systematically sample ecosystem type from the Spanish Forest Map at 1:25000 (SFM25) derived from the fourth Spanish NFI (SNFI4) (Álvarez-González et al., 2014), and SSEBop ET data over the pre- and post-fire short-term time series within each wildfire. We inspected visually the grid to remove sample points with missing data and clearly anomalous ET values resulting from potential cloud-masking algorithm errors (Senay et al., 2020, 2022; Yin et al., 2020). The final dataset consisted of 4658 sampling points. We ruled out the presence of spatial autocorrelation patterns in the ET data base on a Moran's I value equal to 0.031, well-below the Moran's I < 0.1 threshold indicated by Diniz-Filho et al. (2012). We implemented a two-way repeated measures ANOVA (2w-rmANOVA) to assess the influence of ecosystem type on the ET behavior over the time series. The significant interaction between ecosystem type and time, if present, was decomposed using a one-way repeated measures ANOVA (1w-rmANOVA) within each ecosystem type level (broadleaf, conifer and mixed forests, and shrublands). A subsequent Tukey's HSD test was implemented to evaluate whether there were significant differences in ET between the pre-fire scenario (ET_{pre}), immediate post-fire situation (ET_{0-v}), and 1-year after fire (ET_{1-v}). The same procedure (1w-rmANOVA and Tukey's HSD test) was used to assess differences in ET_{pre}, ET_{0-y} and ET_{1-y} among ecosystem types. We tested compliance with repeated measures ANOVA assumptions using diagnostic plots. Statistical significance was determined at the 0.05 level.

3.2. Drivers of post-fire ET reduction

Absolute (aET $_{1-y}$) and relative (rET $_{1-y}$) reduction in ET 1-year after fire was calculated following Eq. 1 and Eq. 2:

$$aET_{1-y} = \left(ET_{pre} - ET_{1-y}\right) - \left(ET_{pre}^{c} - ET_{1-y}^{c}\right)$$
(2)

$$rET_{1-y} = \left(aET_{1-y}/ET_{pre}\right) \times 100 \tag{3}$$

where $\mathrm{ET}_{\mathrm{pre}}$ and ET_{1-y} correspond to the ET for burned areas in the prefire situation and 1-year after fire, respectively. $\mathrm{ET}_{\mathrm{pre}}^{c}$ and ET_{1-y}^{c} denote ET in unburned control areas for the same time periods. Following Ma et al. (2020), we used unburned control areas to isolate fire-induced changes, similar to the widely-used offset term in the dNBR index (Parks et al., 2014). For each fire severity reference plot and ecosystem type (see Section 3.2.1), mean $\mathrm{ET}_{\mathrm{pre}}^{c}$ and ET_{1-y}^{c} were extracted in homogeneous areas outside the fire scar and selected based on three criteria: 1) they were located within the same watershed; 2) they were dominated by the same ecosystem type; and 3) they fell within the same 100-m elevation bin.

Based on previous studies (e.g. Boisramé et al. 2019; Quintano et al., 2020), we used Random Forest (RF) regression (Breiman, 2001) to highlight how the rET1-y is shaped by fire severity, pre-fire ecosystem conditions, and topographic and climatic factors.

3.2.1. Environmental predictors

We disentangled the behavior of fire-induced rET_{1-y} in response to the variability of fire severity along with ten biophysical attributes related to the pre-fire vegetation type/structure and topographical context (Table 3). We adopted a stratified random experimental design (Congalton and Green, 2009) to establish 240 30 m \times 30 m plots within the four wildfires to use as fire severity reference data, i.e. ground reference (71 low fire severity plots, 89 moderate fire severity plots, and 80 high fire severity plots), using the ecosystem type as strata. The SFM25 was used to identify the area occupied by each ecosystem type within the wildfires, and to extract the ecosystem type for each reference plot. We leveraged the SSEBop ET grid to establish the plots and SPOT 6 and 7 images provided by the Copernicus-Emergency Management

Table 3 Putative environmental predictors of the relative reduction in evapotranspiration 1-year after fire (rET_{1-y}) considered in the Random Forest (RF) regression algorithm.

GROUP	SOURCE	VARIABLE	ABBREVIATION	UNIT
Fire ecological impact	Copernicus EMS maps	Categorized fire severity	-	-
Pre-fire fuel variables	SNFI4/ SFM25	Ecosystem type	-	-
	Landsat-8	pre-fire fractional vegetation cover	FCOVER	-
	Sentinel-1	pre-fire VH backscatter (structural complexity)	VH	dB
		pre-fire VV backscatter (structural complexity)	VV	dB
Topographical	PNOA DTM	Altitude	-	m
context		Terrain roughness	-	-
		Topographic Position Index	TPI	-
		Compound Topographic Index	CTI	-
		Heat Load Index	HLI	$^{ m MJ}$ $^{ m cm}^{-2}$ $^{ m year}^{-1}$
		Site Exposure Index	SEI	-

Copernicus EMS: Copernicus Emergency Management Services; PNOA DTM: Digital Terrain Model of the Spanish National Aerial Orthophotography Plan

Service (EMS) at a spatial resolution of 1.5 m to obtain ground-reference categorized fire severity data through expert visual inspection. The labeling of each reference plot (Table 1) was carried out by the predominant fire severity level observed within the plot. Following Quintano et al. (2013), we assigned a reference plot as having burned at low fire severity if it had a dead tree proportion lower than 50 %, at moderate fire severity if the proportion ranged between 50 % and 90 %, and at high fire severity if the proportion was higher than 90 %.

We inverted the PROSAIL-D RTM (Jacquemoud et al., 2009), which couples the PROSPECT-D leaf hemispherical transmittance and reflectance model (Féret et al., 2017) and the 4SAIL canopy reflectance model (Verhoef et al., 2007), to retrieve pre-fire fractional vegetation cover (FCOVER) at a spatial resolution of 30 m in Google Earth Engine (Gorelick et al., 2017) from a Landsat-8 Operational Land Imager (OLI) Level 2, Collection 2, Tier 1 atmospherically corrected scene. We selected the same scene date (July 8th, 2022) as the SSEBop ET_{pre} product. The PROSAIL-D RTM was used to simulate top-of-canopy spectral reflectance and the corresponding FCOVER considering prior knowledge on the physicochemical plant traits of the species assemblage in the study sites to parametrize the PROSPECT-D and 4SAIL models (see Fernández-Guisuraga et al., 2021a, 2021b, 2023a for more details). We addressed the effect of mixed spectral signals at subpixel level by applying a linear spectral mixing model, which takes into account vegetation and soil endmember fractions (Fernández-Guisuraga et al., 2021a). A Latin hypercube sampling design was used to select a total of 10,000 combinations of the variable space as defined by the ranges of PROSAIL-D RTM input parameters. Then, we ran PROSAIL-D RTM in forward mode to generate a FCOVER and reflectance simulation dataset in the optical domain (400-2500 nm by 1 nm), which was resampled to the Landsat-8 OLI band configuration using the sensor spectral response function and band width. The simulation dataset was uploaded to GEE for conducting the PROSAIL-D RTM inversion. The RF regression ensemble learning algorithm was used to construct the relationships between the FCOVER and the corresponding reflectance in the Landsat-8 OLI band configuration. The default hyperparameter values for the RF implementation in GEE were preserved, except for the number of trees, which was set to 500 to improve retrieval efficiency. The trained RF model was then applied to the observed Landsat-8 OLI reflectance in the pre-fire scene to retrieve pixel-based FCOVER.

In this study, we leveraged the sensitivity of synthetic aperture radar (SAR) backscatter to the density and size distributions of stems, branches, and foliage throughout the canopy vertical profile (Bergen et al., 2009), particularly under the typical canopy architecture and closure of Mediterranean forest and shrubland ecosystems (Belenguer-Plomer et al., 2019). Therefore, we acquired a Sentinel-1 C-band SAR scene (July 12th, 2022) in GEE as a proxy for pre-fire vegetation structural complexity (Fernández-Guisuraga et al., 2023b; Jimeno-Llorente et al., 2023). The Sentinel-1 scene corresponded to a Level-1 Ground Range Detected (GRD) product acquired at dual polarization (transmitter-receiver VV + VH) in interferometric wide swath mode. Level-1 GRD products in GEE are already processed to gamma naught (γ^0) backscatter coefficients in dB units at a spatial resolution of 10 m from the following steps: (i) removal of invalid data and low intensity noise on Sentinel-1 scene borders, (ii) thermal noise removal, (iii) radiometric calibration to compute radar brightness from sensor calibration parameters, and (iv) terrain correction (i.e. orthorectification) using 30-m Shuttle Radar Topography Mission (SRTM30) elevation data (GEE, 2023).

Although not validated with field data, the pre-fire FCOVER is an intrinsic vegetation biophysical property featuring a direct and mechanistic link with field-based descriptors of fire behavior and post-fire ecosystem functioning (De Santis and Chuvieco, 2009; Peters et al., 2021; Fernández-Guisuraga et al., 2023a, 2023c), which has been applied in many previous applied remote sensing and fire ecology-based studies (e.g. Fernández-García et al., 2022; Beltrán-Marcos et al., 2023). In this context, FCOVER retrievals through the PROSAIL-D RTM have been extensively validated in many burned and non-burned Mediterranean ecosystems (e.g. Fernández-Guisuraga et al., 2021a, 2021b, 2023a, 2023c), showing a high overall fit ($R^2 = 0.84-0.96$), and, thus, we can expect here a similar FCOVER retrieval performance for this study (De Santis and Chuvieco, 2007). The same rationale can be extended to the use of Sentinel-1 VV and VH backscatter as a proxy for pre-fire vegetation structural complexity (VH would give be related to volumetric scattering while VV would be more sensitive to surface scattering). These two variables may characterize the variability in the crown, volumetric and dihedral scattering in forest and shrubland ecosystems (e.g. Kalogirou et al., 2014; Jimeno-Llorente et al., 2023).

To evaluate topographic effects, the following variables were included in the study (Table 3): altitude and terrain roughness; the latter is often used as a proxy for topographic complexity based on the variability in surface height within a landscape (Riley et al., 1999). Roughness variables included the topographic position index (TPI); the compound topographic index (CTI); heat load index (HLI); aridity index (AI); and the site exposure index (SEI). The TPI calculates the relative elevation of a target pixel compared to its surrounding pixels (Guisan et al., 1999). Positive TPI values suggest that the pixel is positioned higher than its neighbors, typically evidencing ridge tops or elevated areas. In wildfire scenarios, this elevation difference can contribute to fuel pre-heating through convection, as the elevated terrain may facilitate heat rising from the fire, potentially drying and pre-heating vegetation ahead of the fire front, increasing its intensity and spread. The CTI is closely related to the potential for water retention or drainage within a landscape. Areas with high CTI tend to retain water, due to the shape of the land (valleys and depressions), while low CTI areas, such as ridges or slopes, allow water to evacuate quickly. This concept is crucial in fire models, as it helps predict moisture availability, which influences fire behavior and recovery processes after wildfires (Gessler et al., 1995). The HLI was employed as a surrogate for evapotranspiration and soil temperature in this study. It was calculated using the method outlined

by McCune and Keon (2002), which is designed to estimate heat load on a given site by considering factors such as slope, aspect, and latitude. This index helps to predict the amount of solar radiation received by the surface, influencing both evapotranspiration rates and soil temperature, which are crucial for understanding post-fire recovery dynamics in ecosystems. Finally, the SEI estimates relative solar exposure by adjusting the aspect of a terrain to a north-south axis and accounting for the steepness of the slope. This method allows for the quantification of how terrain features affect solar radiation exposure, which can influence processes such as plant growth and fire behavior. The method was described by Balice et al. (2000), where the relative solar exposure is used to understand environmental conditions affecting vegetation and ecosystem processes.

3.2.2. ET reduction analysis

The relative reduction in ET 1-year after fire (rET_{1-y}) and their environmental variables related to the wildfire ecological impact, prefire vegetation type/structure and topographical context were extracted for each fire severity reference plot following the approach of Picotte and Robertson (2011). For this purpose, we sampled within each plot a systematic grid of 20 points with 5-m spacing to (i) minimize the possible mismatch between the plot edges and the grid size of several environmental variables in data extraction, and (ii) circumvent the use of data resampling techniques. We fitted a two-way ANOVA (2w-ANOVA) and subsequent Tukey's HSD test to investigate the effects of fire severity and ecosystem type, as well as their interaction, on the relative reduction in evapotranspiration 1-year after fire (rET_{1-y}). We tested compliance with ANOVA assumptions using diagnostic plots. Statistical significance was determined at the 0.05 level.

The RF regression was used to disentangle the relative contribution of fire severity, pre-fire vegetation type/structure and topographical variables (predictors; Table 3) on the rET1-y outcome (dependent variable). We chose the RF algorithm because it can detect both complex non-linear responses and interactions among the predictors, minimizes overfitted issues and is not very sensitive to multicollinearity (Breiman, 2001; Cutler et al., 2007; Belgiu and Drăgut, 2016; Gigović et al., 2019; Quintano et al., 2023). The Boruta feature selection technique (Kursa and Rudnicki, 2010), designed as a RF wrapper algorithm based on permutation tests for computing variable importance measures using a holdout approach (Hornero et al., 2021), was used to select non-redundant features within the environmental predictors' dataset and thus improve RF model interpretability and predictive performance (Speiser et al., 2019). In the Boruta algorithm, variable importance measures (Z-scores) against shadow variables are calculated to label predictors as unimportant, tentative and important (Kursa and Rudnicki, 2010). We retained in the RF regression algorithm predictors labeled as important by the Boruta algorithm. The optimum RF mtry hyperparameter value was determined through 10-fold cross-validation tuning, while we set the value of the ntree hyperparameter at 2000 to secure stable predictions (Probst and Boulesteix, 2018). The rET_{1-v} variance explained by the RF model (pseudo-R²) was assessed through the internal out-of-bag error rate, and predictive performance through the mean absolute error (MAE), the root mean squared error (RMSE), and the mean bias error (MBE). The relationship between rET_{1-v} and each continuous predictor included in the RF model was screened by using partial dependence plots. The H-statistic (Friedman and Bogdan, 2008) was used to examine the overall interaction strength per environmental predictor (H_i) and pairwise interactions (H_{i,k}) as a proxy for the RF explained variability by predictor interactions rather than by their main effects. The strongest pairwise interactions were screened by using three-dimensional partial dependence plots.

All analyses were implemented in R (R Core Team, 2021) using the rstatix (Kassambara, 2022), Boruta (Kursa and Rudnicki, 2010), RandomForest (Liaw and Wiener, 2002), caret (Kuhn, 2020), pdp (Greenwell, 2017), iml (Molnar et al., 2018) and plotmo (Milborrow, 2022) packages.

4. Results

4.1. ET evolution in the short-term after fire

All ecosystem types systematically sampled within each wildfire showed a sharp and consistent pattern of ET reduction as estimated by the SSEBop product during the first months after fire, followed by a gradual recovery throughout the following year (Fig. 2). Reduction of ET in the immediate post-fire scenario (ET $_{0-y}$) relative to the pre-fire ET values (ET $_{pre}$) averaged 2.09 mm in broadleaf forests, 2.15 mm in conifer forests, 2.03 mm in mixed forests, and 2.61 mm in shrublands (Fig. 2). Although the ET had not recovered in the short-term after fire in each ecosystem (Table 4), the extent of ET recovery throughout the time series was dependent on ecosystem type, as shown by the significant interaction between ecosystem type and time (*p-value* < 0.001) in the 2w-rmANOVA. Importantly, broadleaf forests showed higher ET 1-year after fire (ET $_{1-y}$) than the other forest and shrubland ecosystems. There were no differences in ET $_{pre}$ and ET $_{0-y}$ between broadleaf and conifer forests (Fig. 2 and Table 4).

4.2. Drivers of post-fire ET reduction

In the fire severity reference plots, the highest relative reduction in evapotranspiration 1-year after fire (rET_{1-y}) was found in conifer forests, followed by shrublands and broadleaf forests. In mixed forests, the rET_{1-y} did not differ from that in broadleaf forests and shrublands (Fig. 3). The interaction between fire severity and ecosystem type was not significant (Table 5). Indeed, the effect of fire severity on the rET_{1-y} followed the same behavior within each ecosystem (Fig. 3). The rET_{1-y} was more pronounced for areas that burned at high fire severity than at low to moderate severity. No significant differences in rET_{1-y} were found between the latter two fire severity scenarios (Fig. 3).

Seven out of eleven environmental variables related to the wildfire ecological impact, pre-fire fuel, and topography included in Table 3 were non-redundant and deemed as important rET_{1-y} predictors by the Boruta algorithm in the reference plots (Fig. 4). Fire severity and pre-fire FCOVER were the most important variables, with a mean Z-score higher than 20. The remaining variables with a higher importance than the Boruta *shadowMax* internal variable were the ecosystem type, pre-fire Sentinel-1 VH and VV backscatter as a proxy for vegetation structural complexity, SEI, TPI and roughness. Their contribution ranged from a Z-score of 7.2–13.5. The retrieval of rET_{1-y} in the reference plots from the

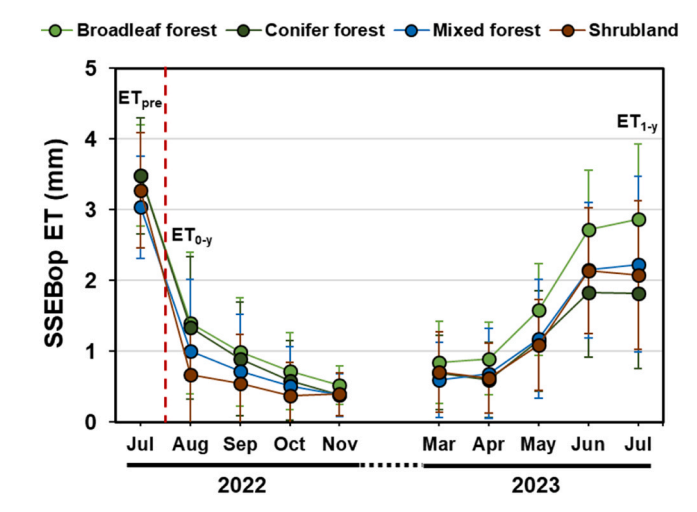


Fig. 2. Mean and standard deviation of the evapotranspiration (ET) as estimated by the SSEBop product systematically sampled within each wildfire in the pre-fire scenario ($ET_{\rm pre}$), immediately post-fire (ET_{0-y}), and throughout the short-term post-fire time series up to 1-year after fire (ET_{1-y}) for broadleaf, conifer and mixed forests, and shrublands.

Table 4Effect of ecosystem type on the evapotranspiration (ET) during the first year post-fire as estimated by the SSEBop product systematically sampled within each wildfire.

2w-rmANOVA	Predictor	F-value	p-value
	Ecosystem type	22.16	< 0.001
	Time (ET _{pre} ,ET ₀ .	3933.17	< 0.001
	_y ,ET _{1-y})		
	Ecosystem type:	133.91	< 0.001
	Time		
1w-rmANOVA (predictor: time)	Ecosystem type	F-value	p-value
	Broadleaf forest	2446.63	< 0.001
	Conifer forest	2775.12	< 0.001
	Mixed forest	724.48	< 0.001
	Shrubland	4393.10	< 0.001
Tukey's HSD	ET _{0-y}	ET_{1-y}	
Broadleaf forest	ET_{pre} < 0.001	< 0.001	
Conifer forest	ET_{pre} < 0.001	< 0.001	
Mixed forest	ET_{pre} < 0.001	< 0.001	
Shrubland	ET_{pre} < 0.001	< 0.001	
1w-rmANOVA (predictor:	Time	F-value	p-value
ecosystem type)			
	ET_{pre}	25.83	< 0.001
	ET _{0-y}	81.80	< 0.001
	ET _{1-y}	44.67	< 0.001
Tukey's HSD (ET _{pre})	Conifer forest	Mixed	Shrubland
		forest	
Broadleaf forest	0.875	< 0.001	0.001
Conifer forest		< 0.001	0.001
Mixed forest			< 0.001
Tukey's HSD (ET _{0-y})	Conifer forest	Mixed	Shrubland
		forest	
Broadleaf forest	0.135	< 0.001	< 0.001
Conifer forest		< 0.001	< 0.001
Mixed forest			< 0.001
Tukey's HSD (ET _{1-y})	Conifer forest	Mixed	Shrubland
		forest	
Broadleaf forest	< 0.001	< 0.001	< 0.001
Conifer forest		< 0.001	< 0.001
Mixed forest			0.138

 $\mathrm{ET}_{\mathrm{pre}}.$ pre-fire scenario; $\mathrm{ET}_{0\text{-y}}.$ immediately post-fire scenario $\mathrm{ET}_{1\text{-y}}.$ 1-year after fire

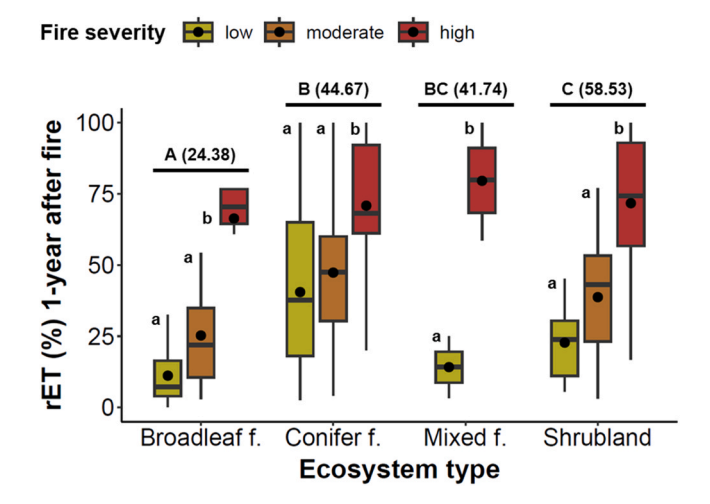


Fig. 3. Boxplot depicting the relationship between fire severity and the relative reduction in evapotranspiration 1-year after fire (reT_{1-y}) by ecosystem type in the fire severity reference plots. Uppercase letters denote significant differences in the mean reT_{1-y} (in parentheses) between ecosystem types. Lowercase letters denote significant differences in the mean $retent{ET}$ between fire severity categories within each ecosystem type. Statistical significance was determined at the 0.05 level.

Table 5Effect of fire severity and ecosystem type on the relative reduction in evapotranspiration 1-year after fire (rET_{1-y}) in the fire severity reference plots.

Predictor	Degrees of freedom	Sum of squares	F- value	p-value
Fire severity (S)	2	68,558	63.159	< 0.001
Ecosystem type (E)	3	38,684	23.762	< 0.001
$S \times E$	5	4215	1.553	0.174

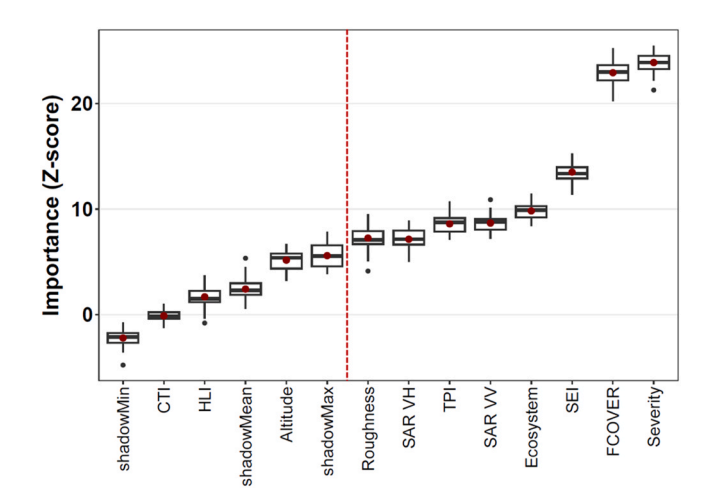


Fig. 4. Ranking of variable importance for predicting the relative reduction in evapotranspiration 1-year after fire (rET_{1-y}) as determined by the Z-score in the Boruta algorithm in the fire severity reference plots. Variables with a Z-score exceeding that of the *shadowMax* internal variable were deemed important (right side of the red dashed line).

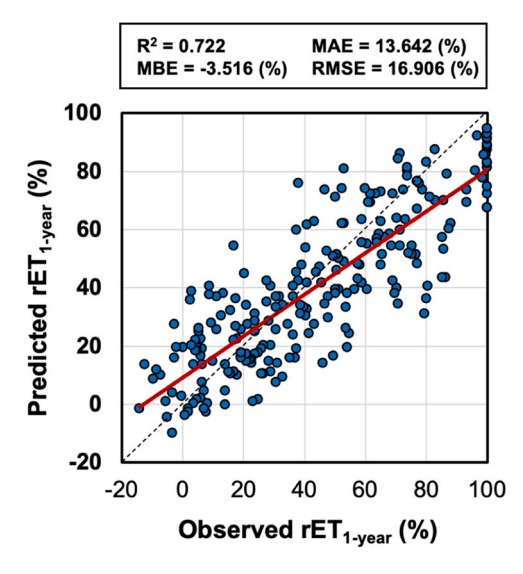


Fig. 5. Relationship between observed and predicted relative reduction in evapotranspiration 1-year after fire (rET_{1-y}) in the reference plots using random forest (RF) regression.

Boruta-selected environmental predictors using RF regression (Fig. 5) featured high overall fit ($pseudo-R^2=0.722$) and relatively low predictive error (RMSE = 16.906 %). The rET_{1-y} retrievals were slightly underestimated (MBE = -3.516 %).

The rET_{1-y} decreased markedly in areas with high pre-fire vegetation cover and structural complexity as determined by the FCOVER and Sentinel-1 backscatter (VH and VV) behavior, respectively (Fig. 6). It

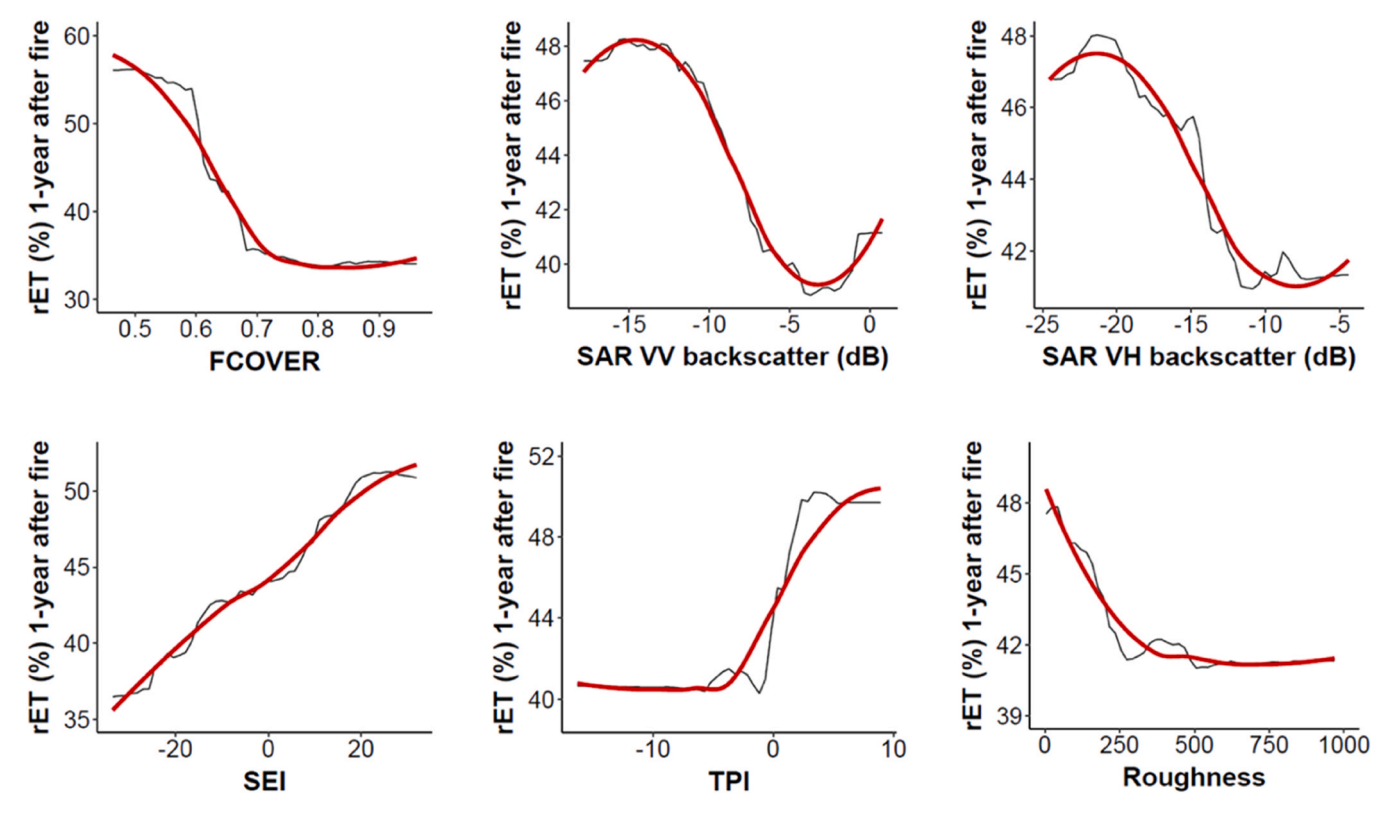


Fig. 6. Partial dependence plots for the continuous predictors of the relative reduction in evapotranspiration 1-year after fire (rET_{1-y}) in the reference plots using random forest (RF) regression, with LOESS smooth curves fitted (red lines).

showed a negative relationship with FCOVER up to 0.7, while it was insensitive to increases in FCOVER above that value. Low terrain roughness and high SEI values, together with positive TPI values, were associated with higher rET_{1-y} (Fig. 6). See Fig. 3 for the effect of fire severity and ecosystem type on rET_{1-y} .

The rET_{1-y} behavior varied markedly in response to the interaction between the environmental predictors in the RF model (Table 6). About 40 % of rET_{1-y} prediction variability is not explained by the sum of all predictor main effects but by their interactions (H = 0.397). The pre-fire FCOVER was the predictor most heavily involved in interactions with other variables (H_j = 0.201), i.e. the FCOVER interactions with other predictors are responsible for about 20 % of the rET_{1-y} variability (Table 6). The H_j value for the next four predictors with the highest interaction strength (fire severity, VV backscatter, terrain roughness and SEI) ranged from 0.147 to 0.171 (Table 6). The strongest pairwise interactions (H_{j,k}) involving these five variables (Table 6) are described through three-dimensional partial dependence plots in Fig. 7. High terrain roughness and pre-fire vegetation structural complexity as measured by VV backscatter constrained rET_{1-y}, but this effect was more apparent in broadleaf and mixed forests than in conifer forests and

shrublands. The rET $_{1-y}$ was somewhat insensitive to terrain roughness in areas burned with high fire severity. Minor rET $_{1-y}$ were predicted in areas where high pre-fire FCOVER coincided with high VV backscatter and low SEI.

5. Discussion

Regarding the influence of ecosystem type on the short-term evolution of post-fire ET values, ET values immediately following fire showed varying degrees of decline across ecosystem types, primarily due to differences in the physiological traits, water use strategies of the dominant vegetation species, and regrowth of fire-adapted vegetation (Poulos et al., 2021; Ma et al., 2020). Our study supports prior findings that wildfires lead to a decrease in ET (Li and Lawrence, 2017; Roche et al., 2020; Collar et al., 2023; Meili et al., 2023), including Mediterranean ecosystems (Sánchez et al., 2015; Häusler et al., 2018; Fernández-Manso et al., 2020; Quintano et al., 2024). Decrease in ET following a wildfire is largely driven by a reduction in leaf cover (Seidl et al., 2014; Liu et al., 2019), and to a lesser degree by the post-fire vegetation type (Li and Lawrence, 2017; Niemeyer et al., 2020). Fire-induced alterations

Table 6 Interaction strength as measured by the H-statistic for the environmental predictors of evapotranspiration 1-year after fire (rET_{1-y}) in the random forest (RF) model. The five strongest overall interactions per feature (H_i) and pairwise interactions ($H_{i,k}$) are highlighted in bold.

H_j	Ecosystem	severity	FCOVER	VH	VV	roughness	TPI	SEI
	0.101	0.167	0.201	0.127	0.147	0.154	0.132	0.171
$H_{j,k}$	Ecosystem	severity	FCOVER	VH	VV	roughness	TPI	SEI
Ecosystem		0.094	0.073	0.111	0.164	0.226	0.070	0.087
severity			0.055	0.031	0.070	0.158	0.107	0.129
FCOVER				0.078	0.160	0.107	0.057	0.140
VH					0.039	0.127	0.106	0.076
VV						0.093	0.103	0.119
roughness							0.069	0.069
TPI								0.097

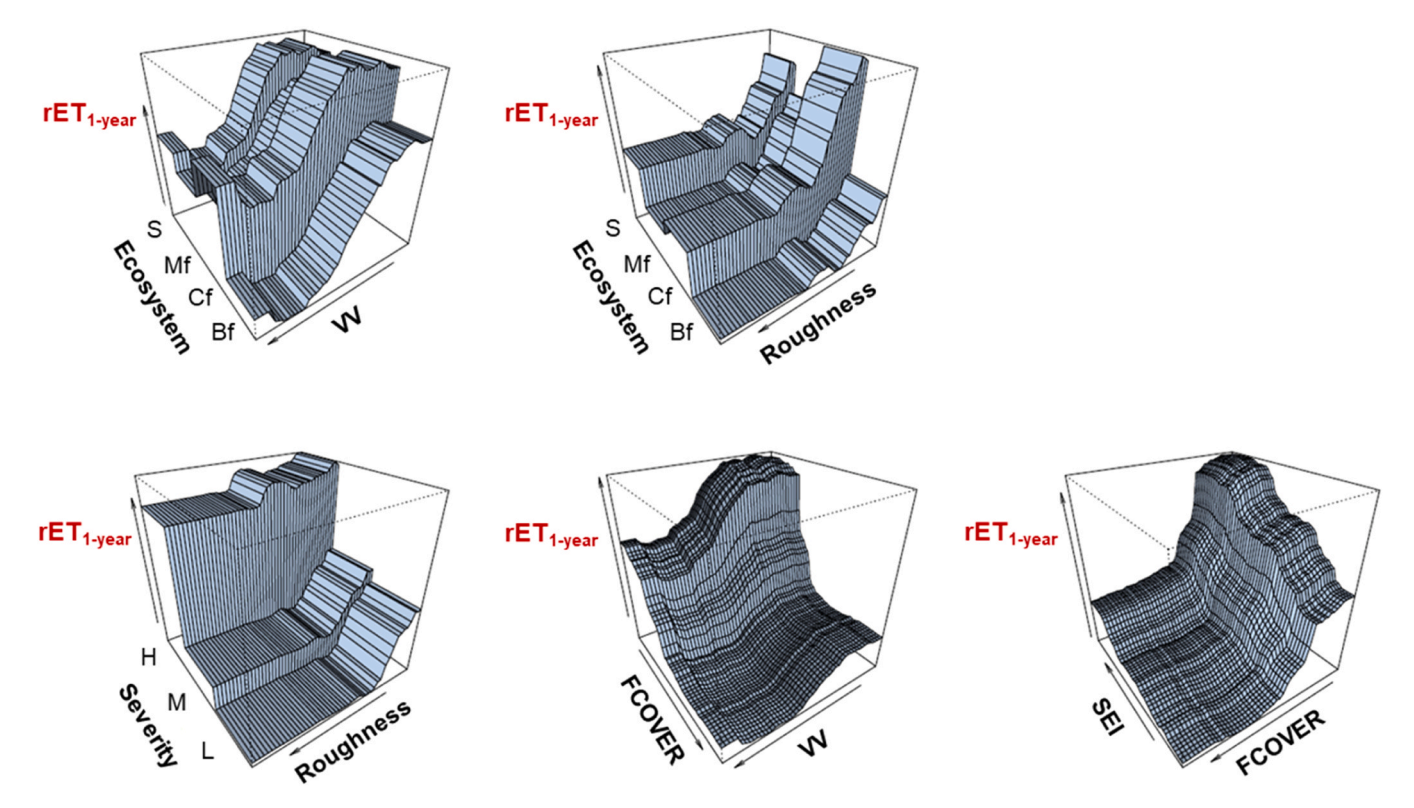


Fig. 7. Three-dimensional partial dependence plots depicting the five strongest pairwise interactions between environmental predictors of evapotranspiration 1-year after fire (rET_{1-v}) in the random forest (RF) model. Table 6 displays the size of interactions.

in vegetation structure and composition can significantly influence post-fire water dynamics (Bond-Lamberty et al., 2009), affecting how ecosystems regulate ET and recover after fire (Blount et al., 2020, Ma et al., 2020).

Our results revealed that conifer forests exhibited the greatest relative reduction in ET 1-year after fire (rET₁-v), followed by shrublands. This pattern contrasts in part with previous studies (e.g., Poulos et al., 2021), which reported comparatively smaller post-fire ET declines in shrublands, typically attributed to their rapid resprouting capacity. However, in our study area, shrubland communities are composed of both resprouting and obligate seeder species. These functional groups rely on distinct post-fire survival strategies, whose success is strongly influenced by the characteristics of the local fire regime (Paula and Pausas, 2006; Fernández-García et al., 2020). By the contrary, broadleaf forests of our study areas are mainly resprouters what might explain the higher ET 1-year after fire. Our study also showed that the reduction in ET 1-year after fire (rET_{1-v}) was strongly influenced by fire severity. The decrease was significantly greater in high-severity areas compared to low-to-moderate severity areas, which is consistent with previous studies (Nolan et al., 2015; Häusler et al., 2018; Mankin and Patel, 2023; Quintano et al., 2024). This pattern reinforces the idea that the extent of damage to vegetationhas a lasting impact on the recovery of transpiration and overall water balance (Wine and Cadol, 2016). High-severity fires can cause long-lasting reductions in ET, sometimes for years or even decades, as ecosystems recover from fire damage (Dore et al., 2010; Poulos et al., 2021; Mankin and Patel, 2023). In high-severity areas, fires kill most aboveground vegetation, which leads to decreased leaf surface area for transpiration, increased soil evaporation, and higher surface runoff, particularly in the short-term after the fire (Poon and Kinoshita, 2018). Fire severity also changes local environmental conditions, such as increasing solar radiation and vapor pressure deficits, which directly influence soil evaporation (Aguilar et al., 2010). As a result, ecosystems recovering from high-severity fires often experience reduced transpiration (T), increased evaporation (E), and shifts in the water and carbon balance, with heightened runoff and stream flow (Wine and Cadol, 2016).

Following fire severity, pre-fire FCOVER emerged as the second most important variable in predicting post-fire ET dynamics (rET_{1-v}). Incorporating pre-fire FCOVER as a biophysical driver for modeling fire-induced changes in ET is a novel approach. Although previous studies identified tree canopy cover as a driver of post-fire ET (e.g. Poulos et al., 2021) they rely on empirical methods (e.g. spectral indices or machine learning algorithms calibrated with field data) that may have transferability issues and low performance in heterogeneous vegetation assemblages and with high bare soil cover (Rigge et al., 2020; Fernández-Guisuraga et al., 2021a). Conversely, FCOVER retrieved from optical imagery by the inversion of RTMs is a physically and ecologically meaningful variable with proven effectiveness and high transferability when monitoring heterogeneous vegetation assemblages across distinct environmental contexts (e.g. Campos-Taberner et al., 2016; Fernández-Guisuraga et al., 2021a). FCOVER has also been used in the fire ecology literature to predict the likelihood of extreme fire behavior and high fire severity (Fernández-García et al., 2022; Beltrán-Marcos et al., 2024), to evaluate vegetation responses to prescribed burns aimed at reducing fire severity (Fernández-Guisuraga and Fernandes, 2024), and to assess post-fire vegetation recovery (Lazzeri et al., 2021). Fernández-Guisuraga et al. (2023c) used the FCOVER recovery as a resilience indicator of vegetation, when studying geophysical drivers of post-fire vegetation recovery. Lastly, FCOVER has also been used as a biophysical indicator of fire severity, yielding promising results (Fernández-Guisuraga et al., 2023a). In that study, the FCOVER metric (ratio of post-fire to pre-fire FCOVER) provided more accurate CBI estimations ($R^2 = 0.87 \pm 0.04$) than conventional spectral indices (as dNBR and relativized versions) and a better transferability performance (nRMSE = 14.27 % \pm 3.75 %) than that of the spectral indices (nRMSE = 21.97 % \pm 8.09 %). These applications highlight the FCOVER relevance in understanding the long-term impacts of fire on ecosystems and water balance.

Among other important variables for predicting rET_{1-v} were ecosystem type and pre-fire vegetation structural complexity (represented by SAR VV and SAR VH). The rET_{1-v} closely related to the ET recovery rate was different in each ecosystem (specially, in low and moderate fire severity areas), which is in accordance with previous research findings (e.g. Yuan et al., 2010; Poulos et al., 2021; Collar et al., 2023). No previous studies have directly linked pre-fire vegetation structural complexity with changes in ET post-fire. However, there is a recognized and significant, complex relationship between pre-fire vegetation structure and post-fire ET. The structural complexity of vegetation prior to a fire, which includes factors like density and canopy height, is known to significantly influence fire severity (García-Llamas et al., 2019b). Denser, taller canopies often create specific microclimates, influencing humidity, temperature, and light availability (Jucker et al., 2018; Davis et al., 2018), all of which affect ET processes. Denser, taller canopies can reduce soil evaporation by shading the ground, increase transpiration by providing more leaf area for water loss, and reduce wind speed and increase humidity within the canopy, which can either enhance or reduce ET depending on other conditions (Xu et al., 2024). In summary, the complexity and characteristics of vegetation structure play a crucial role in determining the rates and patterns of evapotranspiration in an ecosystem (Poca et al., 2018). This trend becomes even more pronounced when considering the strong interactions between vegetation structural complexity, FCOVER and ecosystem type in this study. Post-fire ET was significantly related to plant species composition. Each ecosystem has unique characteristics that influence how quickly ET rates can return to pre-fire levels (Mankin and Patel, 2023). In our fire severity reference plots, we observed that the largest immediate post-fire reduction in evapotranspiration (rET_{0-v}) occurred in plots located in shrublands. However, beginning in the following spring, the faster regeneration of shrublands and broadleaf forests compared to conifer forests resulted in a greater rET_{1-y} in the plots located in conifer forest. In forested areas, high-severity fires can lead to a significant reduction in ET due to the extensive loss of tree canopy and understory vegetation. Recovery in these ecosystems can take many years, depending on the species and environmental conditions (Zalman et al., 2023). In shrub-dominated ecosystems, the response to fire severity can vary widely. Low-severity fires may have minimal impact on ET, while high-severity fires can significantly reduce ET by destroying aboveground biomass. The recovery of ET in these areas depends on the resilience and regrowth rate of shrub species (Wasserman and Mueller, 2013). In our study, both shrublands and broadleaf forests are dominated by resprouting species, which likely facilitated their rapid recovery, in contrast to conifer forests, composed of obligate seeders that regenerate more slowly. Moreover, the fact that the highest rET₁-y was observed in conifer forests is consistent with the finding that rET₁-y showed the greatest decrease in areas with high pre-fire vegetation cover and structural complexity, as indicated by FCOVER and Sentinel-1 backscatter (VH and VV) predictors.

Three topographical variables emerged as key predictors of rET_{1-v}, highlighting the significant role of terrain in influencing ET recovery after a wildfire, as previous studies have shown (Ebel, 2013, Nolan et al., 2015; Goeking and Tarboton, 2020; Zhang and Liu, 2022). SEI, which accounts for both slope and solar radiation exposure, ranked as the third most important variable from the total model set. It may reflect how solar radiation impacts plant growth, influences post-fire vegetation recovery and, consequently, ET (Aguilar et al., 2010; Kinoshita and Hogue, 2011; Ebel, 2013). TPI, which is indicative of relative elevation with respect to the surroundings, can determine local conditions like temperature, wind exposure, humidity and soil moisture availability, all of which affect post-fire ET and plant physiological responses (Nolan et al., 2015; Bart et al., 2016). Lastly, terrain roughness showed important interactions with ecosystem type and fire severity, which were the most influential variables for predicting rET1-y. Terrain roughness may influence post-fire ET through its direct control on fire behavior and severity (Fernandes et al., 2016), and by shaping wind

patterns, microclimate, soil moisture distribution and vegetation structure, ultimately controlling water transfer from the land surface and vegetation to the atmosphere (Nolan et al., 2015; Bart et al., 2016).

The availability of high-resolution ET products is enabling studies at local and regional scales with significantly improved accuracy (Sánchez et al., 2015; Ma et al., 2020; Mankin and Patel, 2023; Quintano et al., 2020; Fernández-Manso et al., 2020; Hausler et al., 2018; Collar et al., 2023; Wilder and Kinoshita, 2022), which were previously restricted to empirical ET estimates derived from flux measurements at highly localized field sites (Nolan et al., 2015; Rocha and Shaver, 2011; Clark et al., 2012; Roche et al., 2020). In this regard, our study has demonstrated the suitability of the SSEBop Landsat-based ET product for assessing the short-term impacts of wildfires on ET within Mediterranean Basin ecosystems (Quintano et al., 2024). Our findings indicate that ET products with high temporal and spatial resolution could play a crucial role in advancing our understanding of these effects, especially in the context of increasingly extreme wildfire events (Quintano et al., 2024). However, our research only analyzed the reduction in ET 1-year after the wildfire event. Tracking vegetation recovery over time would be highly beneficial, enabling the analysis of regeneration patterns and evapotranspiration (ET) recovery drivers across the various ecosystems studied. This represents a key area for future research. Additionally, future research could expand beyond Mediterranean ecosystems to test whether our results are applicable to wildfires in other biomes and ecosystems, as the fundamental processes linking ET with post-fire landscape recovery, such as changes in canopy cover, soil exposure, and microclimatic conditions, apply across diverse vegetation and topo-climatic conditions. Similarly, a potential future line of research would involve comparing the results obtained in this study (based on the fine-resolution SSEBop model) with derived those coarser-resolution ET models such as those based on MODIS or ECO-STRESS data. A previous study (see Quintano et al., 2024) found that the simplified SSEBop model produced results comparable to those of the more complex eeMETRIC model. Finally, our findings could benefit from upcoming satellite missions that will provide high-resolution ET imagery on a global scale, and/or will offer opportunities to capture radar and lidar data, such as the NASA-ISRO Synthetic Aperture Radar (NISAR) mission and the BIOMASS series satellites, which can provide detailed information on the biomass and three-dimensional structure of affected ecosystems. Integrating these datasets could enhance the accuracy and applicability of ET monitoring across diverse regions and conditions, allowing for a more detailed understanding of fire impacts on water cycles in various ecosystems. Furthermore, the ability to combine these observations with advanced machine learning models could facilitate the detection of complex recovery patterns in different ecosystem types and under different fire severity conditions, optimizing post-fire management and ecosystem restoration.

The application of the results obtained on the reduction of post-fire ET and the biological and physical factors that influence its recovery may have significant implications for the formulation of ecosystem management and restoration policies in non-Mediterranean biomes. For example, in forests where fires are natural and recurrent events, understanding the relationship between fire severity, pre-fire FCOVER and topography could help design restoration strategies that prioritize the conservation of species with high water retention capacity and fire resistance (Bond-Lamberty et al., 2009). Similarly, where vegetation recovery is rapid, but fires can have severe impacts on biodiversity and water cycles, the use of remotely sensed ET models could facilitate the assessment of areas requiring more intensive restoration interventions. In addition, the implementation of policies using ET and FCOVER assessment could help prioritize resources in wildfire management in areas with high topographic variability, such as mountain ecosystems, where the interaction between topography and fire severity can influence vegetation regeneration and ecosystem service recovery (Nolan et al., 2015). These strategies may include reforestation with native species that provide an optimal balance between ET recovery and fire

resistance, as well as management of water catchment areas to mitigate erosion and maximize infiltration (Ebel, 2013). This study, by identifying fire severity and pre-fire FCOVER as key factors affecting post-fire ET recovery, provides a basis for understanding how these elements could influence ecosystem resilience in a future marked by more extreme and prolonged fires. The role of ET as an indicator of ecosystem health and water availability becomes even more relevant in the context of climate change, where post-fire recovery may be slower and conditions for new fires may emerge more rapidly (Nolan et al., 2015). Prolonged reduction of ET in areas affected by high severity fires can alter the regional water balance, affecting not only ecological processes, but also the human communities that depend on these ecosystems (Wine and Cadol, 2016).

6. Conclusions

By using the SSEBop Landsat-based model, we were able to capture the spatiotemporal dynamics of evapotranspiration (ET) across fire-affected areas during the first post-fire year. Our results provide clear evidence that higher fire severity leads to significant reductions in ET, primarily due to canopy loss and associated changes in microclimatic conditions. Among the ecosystems studied, the smallest ET reductions were observed in broadleaf forests, followed by shrublands, likely reflecting their relatively rapid resprouting capacity one year after fire.

While our findings are consistent with previous studies reporting post-fire ET declines across various ecosystem types, the approach adopted in this study is novel in three key aspects: (1) the incorporation of FCOVER as a biophysical driver, (2) the use of SAR data to characterize pre-fire vegetation structure and complexity, and (3) the application of a simplified, Landsat-based ET model. These findings have important implications for understanding ecosystem recovery and resilience in the face of climate change and increasingly frequent extreme wildfire events. By emphasizing the strong link between pre-fire ecosystem type, vegetation structure, and post-fire ET changes, our study contributes valuable insights for informing post-fire management strategies. In particular, our results support the development of interventions aimed at restoring hydrological balance, safeguarding ecosystem services, and minimizing the risk of erosion and further land degradation.

Future research should focus on long-term vegetation succession and the role of different vegetation types in driving ET recovery. Comparative evaluations of ET models with varying levels of complexity and spatial resolution (such as SSEBop, ECOSTRESS-based, and MODIS-based products) would be particularly valuable. Integrating high-resolution remote sensing data with field-based hydrological measurements could improve predictive accuracy and support adaptive management strategies tailored to the ecological and climatic characteristics of Mediterranean landscapes.

CRediT authorship contribution statement

Carmen Quintano: Writing – original draft, Methodology, Investigation, Funding acquisition, Formal analysis, Conceptualization. José Manuel Fernández-Guisuraga: Writing – original draft, Methodology, Investigation, Funding acquisition, Formal analysis, Data curation, Conceptualization. Dar A. Roberts: Writing – review & editing, Supervision, Conceptualization. Alfonso Fernández-Manso: Writing – original draft, Methodology, Investigation, Funding acquisition, Formal analysis, Conceptualization.

Funding

This study was financially supported by the Spanish Ministry of Science and Innovation in the framework of LANDSUSFIRE project (PID2022–139156OB-C21) within the National Program for the Promotion of Scientific-Technical Research (2021–2023) and by the

Regional Government of Castile and León in the framework of the IA-FIREXTCyL project (LE081P23). Alfonso Fernández-Manso and Carmen Quintano were supported as research visitors at VIPER Lab. (University of California, Santa Barbara) by a Spanish Education Ministry grant (Salvador de Madariaga program, codes PRX22/00305 and PRX22/00307, respectively).

Declaration of Competing Interest

The authors declare that they have no known competing financial interests or personal relationships that could have appeared to influence the work reported in this paper.

Data availability

Data will be made available on request.

References

- AEMET-IM (Agencia Estatal de Meteorología, Ministerio de Medio Ambiente y Medio Rural y Marino; Instituto de Meteorologia de Portugal). Air temperature and precipitation (1971–2000). In Iberian Climate Atlas. 2011.
- Aguilar, C., Herrero, J., Polo, M., 2010. Topographic effects on solar radiation distribution in mountainous watersheds and their influence on reference evapotranspiration estimates at watershed scale. Hydrol. Earth Syst. Sci. 14, 2479–2494.
- Ahmad, S.K., Holmes, T.R., Kumar, S.V., Lahmers, T.M., Liu, P.-W., Nie, W., Getirana, A., Orland, E., Bindlish, R., Guzman, A., Hain, C.R., Melton, F.S., Locke, K.A., Yang, Y., 2024. Droughts impede water balance recovery from fires in the Western United States. Nat. Ecol. Evol. 8 (2), 229–238. https://doi.org/10.1038/s41559-023-02266-8
- Alberdi, I., Condés, S., Martínez, J., Martínez, S., de Toda, S., Sánchez, G., Pérez, F., Villanueva, J.A., Vallejo, R., 2010. Spanish national forest inventory. In National Forest Inventories. In: Tomppo, E., Gschwantner, T., Lawrence, M., McRoberts, R.E. (Eds.), Pathways for Common Reporting. Springer, Berlin, Germany, pp. 527–540.
- Allen, R.G., Pereira, L., Smith, M., 1998. Paper 56 Crop evapotranspiration-Guidelines for Computing Crop Water Requirements-FAO Irrigation and Drainage. Food and Agricultural Organization of the U.N, Rome.
- Allen, R.G., Tasumi, M., Trezza, R., 2007. Satellite-based energy balance for mapping evapotranspiration with internalized calibration (METRIC)—Model. J. Irrig. Drain. Eng. 133, 380–394.
- Allen, R.G., Trezza, R., Tasumi, M., Robison, C., Kjaersgaard, J., Kilic, A., 2018. METRIC—Mapping Evapotranspiration at High Resolution Using Internalized Calibration—Applications Manual for Landsat Satellite Imagery. Univ. Ida. Mosc. 187.
- Álvarez-González, J.G., Cañellas, I., Alberdi, I., Gadow, K.V., Ruiz-González, A.D., 2014. National Forest Inventory and forest observational studies in Spain: applications to forest modeling. For. Ecol. Manag. 316, 54–64.
- Anderson, M., Gao, F., Knipper, K., Hain, C., Dulaney, W., Baldocchi, D., Eichelmann, E., Hemes, K., Yang, Y., Medellin-Azuara, J., Kustas, W., 2018. Field-scale assessment of land and water use change over the California Delta using remote sensing. Remote Sens. 10, 889.
- Anderson, M.C., Norman, J.M., Mecikalski, J.R., Otkin, J.A., Kustas, W.P., 2007.
 A climatological study of evapotranspiration and moisture stress across the continental United States based on thermal remote sensing: 1. Model formulation.
 J. Geophys. Res. Atmos. 112.
- Aparício, B.A., Santos, J.A., Freitas, T.R., Sá, A.C.L., Pereira, J.M.C., Fernandes, P.M., 2022. Unravelling the effect of climate change on fire danger and fire behaviour in the transboundary biosphere reserve of Meseta Ibérica (Portugal-Spain). Clim. Change 173 (1–2). https://doi.org/10.1007/s10584-022-03399-8.
- Balice, R.G., Miller, J.D., Oswald, B.P., Edminster, C., Yool, S.R. 2000. Forest surveys and wildfire assessment in the Los Alamos Region; 1998-1999 (No. LA-13714-MS). Los Alamos National Lab, NM (US).
- Bariş, M., Tombul, M., 2024. A review on models, products and techniques for evapotranspiration measurement, estimation, and validation. Environ. Qual. Manag. 34 (1), e22250. DOI: 10.1002/tqem.22250.
- Bart, R.R., Tague, C.L., Moritz, M.A., 2016. Effect of tree-to-shrub type conversion in lower montane forests of the Sierra Nevada (USA) on Streamflow. PLoS One 11, e0161805. https://doi.org/10.1371/journal.pone.0161805.
- Belenguer-Plomer, M.A., Tanase, M.A., Fernandez-Carrillo, A., Chuvieco, E., 2019.
 Burned area detection and mapping using Sentinel-1 backscatter coefficient and thermal anomalies. Remote Sens. Environ. 233, 111345.
- Belgiu, M., Drăgut, L., 2016. Random forest in remote sensing: a review of applications and future directions. ISPRS J. Photogramm. Remote Sens. 114, 24–31.
- Beltrán-Marcos, D., Calvo, L., Fernández-Guisuraga, J.M., Fernández-García, V., Suárez-Seoane, S., 2023. Wildland-urban interface typologies prone to high severity fires in Spain. Sci. Total Environ. 894, 165000.
- Beltrán-Marcos, D., Suárez-Seoane, S., Fernández-Guisuraga, J.M., Azevedo, J.C., Calvo, L., 2024. Fire regime attributes shape pre-fire vegetation characteristics

- controlling extreme fire behavior under different bioregions in Spain. Fire Ecol. 20 (1), 47. https://doi.org/10.1186/s42408-024-00276-w.
- Bergen, K.M., Goetz, S.J., Dubayah, R.O., Henebry, G.M., Hunsaker, C.T., Imhoff, M.L., Nelson, R.F., Parker, G.G., Radeloff, V.C., 2009. Remote sensing of vegetation 3-D structure for biodiversity and habitat: review and implications for lidar and radar spaceborne missions. J. Geophys. Res. 114. G00E06.
- Blount, K., Ruybal, C.J., Franz, K.J., Hogue, T.S., 2020. Increased water yield and altered water partitioning follow wildfire in a forested catchment in the western United States. Ecohydrology 13. 1–15.
- Boisramé, G.F.S., Thompson, S.E., Tague, C., Stephens, S.L., 2019. Restoring a natural fire regime alters the water balance of a Sierra Nevada catchment. Water Resour. Res. 55, 5751–5769.
- Bond-Lamberty, B., Peckham, S.D., Gower, S.T., Ewers, B.E., 2009. Effects of fire on regional evapotranspiration in the central Canadian boreal forest. Glob. Change Biol. 15 (5), 1242–1254. https://doi.org/10.1111/j.1365-2486.2008.01776.x.
- Boucher, J., Beaudoin, A., Hébert, C., Guindon, L., Bauce, E., 2017. Assessing the potential of the differenced Normalized Burn Ratio (dNBR) for estimating burn severity in eastern Canadian boreal forests. Int. J. Wildland Fire 26 (1), 32. https:// doi.org/10.1071/wf15122.
- Breiman, L., 2001. Random forests. Mach. Learn. 45, 5-32.
- Campos-Taberner, M., García-Haro, F.J., Camps-Valls, G., Grau-Muedra, G., Nutini, F., Crema, A., Boschetti, M., 2016. Multitemporal and multiresolution leaf area index retrieval for operational local rice crop monitoring. Remote Sens. Environ. 187, 102–118.
- Chas-Amil, M.L., García-Martínez, E., Touza, J., 2020. Iberian Peninsula October 2017 wildfires: burned area and population exposure in Galicia (NW of Spain). Int. J. Disaster Risk Reduct. 48. https://doi.org/10.1016/j.ijdrr.2020.101623.
- Chas-Amil, M.L., Touza, J., Prestemon, J.P., 2010. Spatial distribution of human-caused forest fires in Galicia (NW Spain). In: Perona, G., Brebbia, C.A. (Eds.), Modelling, monitoring and management of forest fires II, pp. 247–258.
- Chen, D., Fu, C., Hall, J.V., Hoy, E.E., Loboda, T.V., 2021. Spatio-temporal patterns of optimal Landsat data for burn severity index calculations: Implications for high northern latitudes wildfire research. Remote Sens. Environ. 2021 (258), 112393.
- Christopoulou, A., Mallinis, G., Vassilakis, E., Farangitakis, G.-P., Fyllas, N.M., Kokkoris, G.D., Arianoutsou, M., 2019. Assessing the impact of different landscape features on post-fire forest recovery with multitemporal remote sensing data: the case of Mount Taygetos (southern Greece). Int. J. Wildland Fire 28, 521.
- Clark, K.L., Skowronski, N., Gallagher, M., Renninger, H., Schaffer, K., 2012. Effects of invasive insects and fire on forest energy exchange and evapotranspiration in the New Jersey pinelands. For. Meteor. 166, 50–61.
- Collar, N.M., Ebel, B.A., Saxe, S., Rust, A.J., Hogue, T.S., 2023. Implications of fire-induced evapotranspiration shifts for recharge-runoff generation and vegetation conversion in the western United States. J. Hydrol. 621, 129646.
- Congalton, R.G., Green, K., 2009. Assessing the Accuracy of Remotely Sensed Data.

 Principles and Practices, 2nd edition. CRC Press. Taylor & Francis, Boca Ratón.
- R. Core Team. 2021. R: A language and environment for statistical computing. R Foundation for Statistical Computing, Vienna, Austria. URL ⟨https://www.R-project.org/⟩.
- Cutler, D.R., Edwards, T.C., Beard, K.H., Cutler, A., Hess, K.T., Gibson, J., Lawler, J.J., 2007. Random forests for classification in ecology. Ecology 88, 2783–2792.
- Davis, K., Dobrowski, S., Holden, Z., Higuera, P., Abatzoglou, J., 2018. Microclimatic buffering in forests of the future: the role of local water balance. Ecography 42, 1–11. https://doi.org/10.1111/ecog.03836.
- De Santis, A., Chuvieco, E., 2007. Burn severity estimation from remotely sensed data:

 Performance of simulation versus empirical models. Remote Sens. Environ. 108,
 422–435
- De Santis, A., Chuvieco, E., 2009. GeoCBI: A modified version of the Composite Burn Index for the initial assessment of the short-term burn severity from remotely sensed data. Remote Sens. Environ. 113, 554–562.
- Dias Lopes, J., Neiva Rodrigues, L., Acioli Imbuzeiro, H.M., Falco Pruski, F., 2019.
 Performance of SSEBop Model for Estimating Wheat Actual Evapotranspiration in the Brazilian Savannah Region. Int. J. Remote Sens 2019 (40), 6930–6947.
- Diniz-Filho, J.A., Siquiera, T., Padial, A.A., Rangel, T.F., Landeiro, V.L., Bini, L.M., 2012. Spatial autocorrelation analysis allows disentangling the balance between neutral and niche processes in metacommunities. Oikos 121, 201–210.
- Dore, S., Kolb, T.E., Montes-Helu, M., Eckert, S.E., Sullivan, B.W., Hungate, B.A., Kaye, J. P., Hart, S.C., Koch, G.W., Finkral, A., 2010. Carbon and water fluxes from ponderosa pine forests disturbed by wildfire and thinning. Ecol. Appl. 20, 663–683.
- Ebel, B.A., 2013. Simulated unsaturated flow processes after wildfire and interactions with slope aspect. Water Resour. Res. 49, 8090–8107. https://doi.org/10.1002/ 2013wr014129.
- Eidenshink, J., Schwind, B., Brewer, K., Zhu, Z.L., Quayle, B., Howard, S., 2007. A project for monitoring trends in burn severity. Fire Ecol. 3, 3–21.
- Evangelides, C., Nobajas, A., 2020. Red-edge normalised difference vegetation index (NDVI705) from sentinel-2 imagery to assess post-fire regeneration. Remote Sens. Appl. Soc. Environ. 17, 100283. https://doi.org/10.1016/j.rsase.2019.100283.
- FAO. 2023. Remote Sensing Determination of Evapotranspiration—Algorithms, Strengths, Weaknesses, Uncertainty and Best Fit-Forpurpose; FAO: Cairo, Egypt.
- Féret, J.B., Gitelson, A.A., Noble, S.D., Jacquemoud, S., 2017. Prospect-D: towards modeling leaf optical properties through a complete lifecycle. Remote Sens. Environ. 193, 204–215.
- Fernandes, P.M., 2013. Fire-smart management of forest landscapes in the Mediterranean basin under global change. Landsc. Urban Plan. 110, 175–182.
- Fernandes, P.M., Monteiro-Henriques, T., Guiomar, N., Loureiro, C., Barros, A.M.G., 2016. Bottom-up variables govern large-fire size in Portugal. Ecosystems 19, 1362–1375.

- Fernández-García, V., Beltrán-Marcos, D., Fernández-Guisuraga, J.M., Marcos, E., Calvo, L., 2022. Predicting potential wildfire severity across Southern Europe with global data sources. Sci. Total Environ. 829, 154729.
- Fernández-García, V., Marcos, E., Fulé, P.Z., Reyes, O., Santana, V.M., Calvo, L., 2020. Fire regimes shape diversity and traits of vegetation under different climatic conditions. Sci. Total Environ. 716, 137137. https://doi.org/10.1016/j. scitotenv.2020.137137.
- Fernández-Guisuraga, J.M., Calvo, J., Quintano, C., Fernández-Manso, A., Fernandes, P. M., 2023a. Fractional vegetation cover ratio estimated from radiative transfer modeling outperforms spectral indices to assess fire severity in several Mediterranean plant communities. Remote Sens. Environ. 290, 113542.
- Fernández-Guisuraga, J.M., Calvo, L., Quintano, C., Fernández-Manso, A., Fernandes, P. M., 2024b. Linking crown fire likelihood with post-fire spectral variability in Mediterranean fire-prone ecosystems. Int. J. Wildland Fire 33, WF23174. https://doi.org/10.1071/WF23174.
- Fernández-Guisuraga, J.M., Calvo, L., 2023. Fuel build-up promotes an increase in fire severity of reburned areas in fire-prone ecosystems of the western Mediterranean Basin. Fire Ecol. 19, 72. https://doi.org/10.1186/s42408-023-00232-0.
- Fernández-Guisuraga, J.M., Fernandes, P.M., 2024. Enhanced post-wildfire vegetation recovery in prescribed-burnt Mediterranean shrubland: a regional assessment (art. no). For. Ecol. Manag. 561, 121921. https://doi.org/10.1016/j.foreco.2024.121921.
- Fernández-Guisuraga, J.M., Fernandes, P.M., Tárrega, R., Beltrán-Marcos, D., Calvo, L., 2023c. Vegetation recovery drivers at short-term after fire are plant communitydependent in mediterranean burned landscapes. For. Ecol. Manag. 539, 121034.
- Fernández-Guisuraga, J.M., Fernández-Manso, A., Quintano, C., Fernández-García, V., Cerrillo, A., Marqués, G., Cascallana, G., Calvo, L., 2024a. FIREMAP: cloud-based software to automate the estimation of wildfire-induced ecological impacts and recovery processes using remote sensing techniques. Ecol. Inform. 81, 102591.
- Fernández-Guisuraga, J.M., Suárez-Seoane, S., Calvo, L., 2021b. Radiative transfer modeling to measure fire impact and forest engineering resilience at short-term. ISPRS J. Photogramm. Remote Sens. 176, 30-41.
- Fernández-Guisuraga, J.M., Suárez-Seoane, S., Calvo, L., 2023b. Radar and multispectral remote sensing data accurately estimate vegetation vertical structure diversity as a fire resilience indicator. Remote Sens. Ecol. Conserv. 9, 117–132.
- Fernández-Guisuraga, J.M., Verrelst, J., Calvo, L., Suárez-Seoane, S., 2021a. Hybrid inversion of radiative transfer models based on high spatial resolution satellite reflectance data improves fractional vegetation cover retrieval in heterogeneous ecological systems after fire. Remote Sens. Environ. 255, 112304.
- Fernández-Manso, A., Quintano, C., Roberts, D.A., 2019. Burn severity analysis in Mediterranean forests using maximum entropy model trained with EO-1 Hyperion and LiDAR data. ISPRS J. Photogramm. Remote Sens. 155, 102–118.
- Fernández-Manso, A., Quintano, C., Roberts, D.A., 2020. Can Landsat-derived variables related to energy balance improve understanding of burn severity from current operational techniques? Remote Sens. 12 (5), 890.
- Filippelli, S.K., Sloggy, M.R., Vogeler, J.C., Manning, D.T., Goemans, C., Senay, G.B., 2022. Remote sensing of field-scale irrigation withdrawals in the central Ogallala aquifer region. Agric. Water Manag. 271, 107764. https://doi.org/10.1016/j. agwat.2022.107764.
- Fisher, J.B., Tu, K.P., Baldocchi, D.D., 2008. Global estimates of the land–atmosphere water flux based on monthly AVHRR and ISLSCP-II data, validated at 16 FLUXNET sites. Remote Sens. Environ. 112, 901–919.
- Friedman, J.H., Bogdan, E.P., 2008. Predictive Learning via Rule Ensembles. Ann. Appl. Stat. 2, 916–954.
- de la Fuente-Sáiz, D., Ortega-Far, S., Fonseca, D., Ortega-Salazar, S., Kilic, A., Allen, R., 2017. Calibration of METRIC model to estimate energy balance over a drip-irrigated apple orchard. Remote Sens. 9, 670.
- García-Llamas, P., Suárez-Seoane, S., Fernández-Guisuraga, J.M., Fernández-García, V., Fernández-Manso, A., Quintano, C., Taboada, A., Marcos, E., Calvo, L., 2019a. Evaluation and comparison of Landsat 8, Sentinel-2 and Deimos-1 remote sensing indices for assessing burn severity in Mediterranean fire-prone ecosystems. Int. J. Appl. Earth Obs. Geoinf. 80, 137–144. https://doi.org/10.1016/j.jag.2019.04.006.
- García-Llamas, P., Suárez-Seoane, S., Taboada, A., Fernández-Manso, A., Quintano, C., Fernández-García, V., Fernández-Guisuraga, J., Marcos, E., Calvo, L., 2019b. Environmental drivers of fire severity in extreme fire events that affect Mediterranean pine forest ecosystems. For. Ecol. Manag. https://doi.org/10.1016/J. FORECO 2018 10 051
- GEE. 2023. Sentinel-1 Algorithms. (https://developers.google.com/earth-engine/guide s/sentinel1) (Accessed on December 6th, 2023).
- Genanu, M., Alamirew, T., Senay, G., Gebremichael, M., 2016. Remote sensing based estimation of evapo-transpiration using selected algorithms: the case of wonji shoa sugar cane estate. Ethiop. Prepr. 20160800.
- Gessler, P.E., Moore, N.I.D., McKenzie, J., Ryan, P.J., 1995. Soil-landscape modeling and spatial prediction of soil attributes. Int. J. GIS 9, 421–432.
- Gigović, L., Pourghasemi, H.R., Drobnjak, S., Bai, S., 2019. Testing a new ensemble model based on SVM and random forest in forest fire susceptibility assessment and its mapping in Serbia's Tara national park. Forests 10, 408.
- Goeking, S.A., Tarboton, D.G., 2020. Forests and water yield: a synthesis of disturbance effects on streamflow and snowpack in Western coniferous forests. J. For. 118 (2), 172–192. https://doi.org/10.1093/jofore/fvz069.
- Gorelick, N., Hancher, M., Dixon, M., Ilyushchenko, S., Thau, D., Moore, R., 2017. Google earth engine: planetary-scale geospatial analysis for everyone. Remote Sens. Environ. 202, 18–27.
- Greenwell, B.M., 2017. pdp: an R package for constructing partial dependence plots. R. J. 9, 421-436.
- Guisan, A., Weiss, S.B., Weiss, A.D., 1999. GLM versus CCA spatial modeling of plant species distribution. Plant Ecol. 143 (1999), 107–122.

- Han, H., Abitew, T.A., Bazrkar, H., Park, S., Jeong, J., 2024. Integrating machine learning for enhanced wildfire severity prediction: a study in the Upper Colorado River basin. Sci. Total Environ. 952, 175914.
- Häusler, M., Nunes, J.P., Soares, P., Sánchez, J.M., Silva, J.M.N., Warneke, T., Keizer, J. J., Pereira, J.M.C., 2018. Assessment of the indirect impact of wildfire (severity) on actual evapotranspiration in eucalyptus forest based on the surface energy balance estimated from remote-sensing techniques. Int. J. Remote Sens 39, 6499–6524.
- Hiestand, M.P., Tollerud, H.J., Funk, C., Senay, G.B., Fickas, K.C., Friedrichs, M.O., 2024. SSEBop evapotranspiration estimates using synthetically derived landsat data from the continuous change detection and classification algorithm. Remote Sens. 16, 1297. https://doi.org/10.3390/rs16071297.
- Hornero, A., Zarco-Tejada, P.J., Quero, J.L., North, P.R.J., Ruiz-Gómez, F.J., Sánchez-Cuesta, R., Hernandez-Clemente, R., 2021. Modelling hyperspectral- and thermal-based plant traits for the early detection of Phytophthora-induced symptoms in oak decline. Remote Sens. Environ. 263, 112570.
- Ireland, G., Petropoulos, G.P., 2015. Exploring the relationships between post-fire vegetation regeneration dynamics, topography and burn severity: a case study from the montane cordillera ecozones of western Canada. Appl. Geogr. 56, 232–248.
- Jacquemoud, S., Verhoef, W., Baret, F., Bacour, C., Zarco-Tejada, P.J., Asner, G.P., François, C., Ustin, S.L., 2009. PROSPECT + SAIL models: a review of use for vegetation characterization. Remote Sens. Environ. 113, 56–66.
- Jimeno-Llorente, L., Marcos, E., Fernández-Guisuraga, J.M., 2023. The effects of fire severity on vegetation structural complexity assessed using SAR data are modulated by plant community types in mediterranean fire-prone ecosystems. Fire 6, 450.
- Jones, G.M., Tingley, M.W., 2022. Pyrodiversity and biodiversity: a history, synthesis, and outlook. Divers. Distrib. 28, 386–403.
- Joshi, R.C., Jensen, A., Pascolini-Campbell, M., Fisher, J.B., 2024. Coupling between evapotranspiration, water use efficiency, and evaporative stress index strengthens after wildfires in New Mexico, USA (art. no). Int. J. Appl. Earth Obs. Geoinf. 135, 104238. https://doi.org/10.1016/j.jag.2024.104238.
- Jucker, T., Hardwick, S., Both, S., Elias, D., Ewers, R., Milodowski, D., Swinfield, T., Coomes, D., 2018. Canopy structure and topography jointly constrain the microclimate of human-modified tropical landscapes. Glob. Change Biol. 24, 5243–5258. https://doi.org/10.1111/gcb.14415.
- Kalogirou, V., Ferrazzoli, P., Vecchia, A.D., Foumelis, M., 2014. On the SAR Backscatter of Burned Forests: A Model-Based Study in C-Band, Over Burned Pine Canopies. IEEE Trans. Geosci. Remote Sens. 52, 6205–6215.
- Kassambara, A. 2022. rstatix: Pipe-Friendly Framework for Basic Statistical Tests. R package version 0.7.1. (https://CRAN.R-project.org/package=rstatix).
- Keely, J.E. 2009. Fire intensity, fire severity an burn severity: a brief review and suggested usage.
- Key, C.H., Benson, N.C. 2006. Landscape Assessment (LA) Sampling and Analysis Methods; USDA Forest Service General Technical Reports; Rocky Mountain Research Station: Fort Collins, CO, USA,; RMRS-GTR-164-CD.
- Kinoshita, A.M., Hogue, T.S., 2011. Spatial and temporal controls on post-fire hydrologic recovery in Southern California watersheds. Catena 87, 240–252. https://doi.org/ 10.1016/j.catena.2011.06.005.
- Koutsias, N., Karamitsou, A., Nioti, F., Coutelieris, F., 2022. Assessment of fire regimes and post-fire evolution of burned areas with the dynamic time warping method on time series of satellite images—setting the methodological framework in the Peloponnese. Greece. Remote Sens. 14, 5237.
- Kuhn, M. 2020. caret: Classification and Regression Training R package version 60-86 $\langle https://CRANR-projectorg/package=caret \rangle$.
- Kursa, M.B., Rudnicki, W.R., 2010. FeaturE Selection with the Boruta Package. J. Stat. Softw. 36, 11.
- Laipelt, L., Kayser, R.H.B., Fleischmann, A.S., Ruhoff, A., Bastiaanssen, W., Erickson, T. A., Melton, F., 2021. Long-term monitoring of evapotranspiration using the SEBAL algorithm and Google Earth Engine cloud computing. ISPRS J. Photogramm. Remote Sens. 178, 81–96.
- Lazzeri, G., Frodella, W., Rossi, G., Moretti, S., 2021. Multitemporal mapping of post-fire land cover using multiplatform prisma hyperspectral and sentinel-uav multispectral data: Insights from case studies in Portugal and Italy. Sensors 21 (12), 3982 (art. no).
- Li, F., Lawrence, D.M., 2017. Role of fire in the global land water budget during the twentieth century due to changing ecosystems. J. Clim. 30 (6), 1893–1908.
- Li, X., Zhang, H., Yang, G., Ding, Y., Zhao, J., 2018. Post-Fire vegetation succession and surface energy fluxes derived from remote sensing. Remote Sens 10, 1000.
- Liang, S., He, T., Huang, J., Jia, A., Zhang, Y., Cao, Y., Chen, X., Chen, X., Cheng, J., Jiang, B., Jin, H., Li, A., Li, S., Li, X., Liu, L., Liu, X., Ma, H., Ma, Y., Song, D.X., Sun, L., Song, L., 2024. Advancements in high-resolution land surface satellite products: A comprehensive review of inversion algorithms, products and challenges. In: In Science of Remote Sensing, 10. Elsevier B.V. https://doi.org/10.1016/j.srs.2024.100152.
- Liaw, A., Wiener, M., 2002. Classification and regression by RandomForest. R. N. 2, 18-22.
- Lippok, D., Beck, S.G., Renison, D., Gallegos, S.C., Saavedra, F.V., Hensen, I., Schleuning, M., 2013. Forest recovery of areas deforested by fire increases with elevation in the tropical Andes. For. Ecol. Manag 295, 69–76.
- Liu, Z., Ballantyne, A.P., Cooper, L.A., 2019. Biophysical feedback of global forest fires on surface temperature. Nat. Commun. 10, 214.
- Lombao, A., Barreiro, A., Fontúrbel, M.T., Martín, A., Carballas, T., Díaz-Raviña, M., 2020. Key factors controlling microbial community responses after a fire: importance of severity and recurrence. Sci. Total Environ. 741. https://doi.org/10.1016/j. scitotenv.2020.140363.
- Ma, Q., Bales, R.C., Rungee, J., Conklin, M.H., Collins, B.M., Goulden, M.L., 2020. Wildfire controls on evapotranspiration in California's Sierra Nevada. J. Hydrol. 590, 125364.

- Mankin, K.R., Patel, R., 2021. Fire effects on evapotranspiration in the upper Rio Grande Basin using landsat-based SSEBop. ASABE Annu. Int. Virtual Meet. 2101065. https://doi.org/10.13031/aim.202101065.
- Mankin, K.R., Patel, R., 2023. Wildfire burn severity affects postfire shifts in evapotranspiration in subalpine forests. J. Nat. Resour. Agric. Ecosyst. 1 (1), 1–11. https://doi.org/10.13031/jnrae.15438.
- Martinson, E.J.; Omi, P.N. 2013. Fuel treatments and fire severity: A meta- analysis. Res. Pap. RMRS-RP-103WWW. Fort Collins, CO: U.S. Department of Agri- culture, Forest Service, Rocky Mountain Research Station. 38 p.
- McCune, B., Keon, D., 2002. Equations for potential annual direct incident radiation and heat load. J. Veg. Sci. 13, 603–606.
- McShane, R.R., Driscoll, K.P., Sando, R. 2017. A review of surface energy balance models for estimating actual evapotranspiration with remote sensing at high spatiotemporal resolution over large extents: U.S. Geological Survey Scientific Investigations Report 2017–5087, 19 p., https://doi.org/10.3133/sir20175087.
- Meili, N., Beringer, J., Zhao, J., Fatichi, S., 2023. Aerodynamic effects cause higher forest evapotranspiration and water yield reductions after wildfires in tall forests. Glob. Change Biol. https://doi.org/10.1111/gcb.16995.
- Meng, R., Dennison, P.E., Huang, C., Moritz, M.A., D'Antonio, C., 2015. Effects of fire severity and post-fire climate on short-term vegetation recovery of mixed-conifer and red fir forests in the Sierra Nevada Mountains of California. Remote Sens. Environ. 171 311–325.
- Mészároš, I., Miklánek, P., 2009. Influence of vegetation cover on evapotranspiration patterns in mountainous areas. Biologia 64 (3), 610–614 https://doi.org/10.2478/ s11756-009-0098-3.
- Milborrow, S. 2022. plotmo: Plot a Model's Residuals, Response, and Partial Dependence Plots. R package version 3.6.2. (https://CRAN.R-project.org/package=plotmo).
- Ministry for Ecological Transition and the Demographic Challenge (MITECO). (2019). Fourth National Forest Inventory: Galicia. Government of Spain.
- Ministry for Ecological Transition and the Demographic Challenge (MITECO). (2020). Fourth National Forest Inventory: Zamora. Government of Spain.
- Ministry for Ecological Transition and the Demographic Challenge (MITECO). (2021). Fourth National Forest Inventory: León. Government of Spain.
- Molnar, C., Bischl, B., Casalicchio, G., 2018. iml: an R package for interpretable machine learning. J. Open Source Softw. 3, 786.
- Nguyen, H.L., Gelsinari, S., Callow, J.N., Silberstein, R., Thompson, S.E., 2025. Satellite and eddy covariance analysis reveals short-lived evapotranspiration changes after fire in Mediterranean woodland (art. No). J. Hydrol. 653, 132654. https://doi.org/ 10.1016/j.jhydrol.2024.132654.
- Niemeyer, R.J., Bladon, K.D., Woodsmith, R.D., 2020. Long-term hydrologic recovery after wildfire and post-fire forest management in the interior Pacific Northwest. Hydrol. Process. 34 (5), 1182–1197.
- Nolan, R.H., Lane, P.N.J., Benyon, R.G., Bradstock, R.A., Mitchell, P.J., 2015. Trends in evapotranspiration and streamflow following wildfire in resprouting eucalypt
- forests. J. Hydrol. 524, 614–624. https://doi.org/10.1016/j.jhydrol.2015.02.045.

 Norlen, C.A., Hemes, K.S., Wang, J.A., Randerson, J.T., Battles, J.J., Tubbesing, C.L.,
 Goulden, M.L., 2024. Recent fire history enhances semi-arid conifer forest drought
 resistance (art. no). For. Ecol. Manag. 573, 122331. https://doi.org/10.1016/j.
 foreco.2024.122331.
- Parks, S.A., Dillon, G.K., Miller, C.A., 2014. New metric for quantifying burn severity: the relativized burn ratio. Remote Sens. 6, 1827–1844.
- Parra, A., Moreno, J.M., 2018. Drought differentially affects the post-fire dynamics of seeders and resprouters in a Mediterranean shrubland. Sci. Total Environ. 626, 1219–1229. https://doi.org/10.1016/j.scitotenv.2018.01.174.
- Pascolini-Campbell, M., Lee, C., Stavros, N., Fisher, J.B., 2022. ECOSTRESS reveals prefire vegetation controls on burn severity for Southern California wildfires of 2020. Glob. Ecol. Biogeogr. 31 (10), 1976–1989. https://doi.org/10.1111/geb.13526.
- Paula, S., Pausas, J.G., 2006. Leaf traits and resprouting ability in the Mediterranean basin. Funct. Ecol. 20 (6), 941–947.
- Pausas, J.G., Keeley, J.E., 2014. Evolutionary ecology of resprouting and seeding in fireprone ecosystems. N. Phytol. 204 (1), 55–65. https://doi.org/10.1111/nph.12921.
- Peters, D.L., Niemann, K.O., Skelly, R., 2021. Remote Sensing of Ecosystem Structure—Part 2: Initial Findings of Ecosystem Functioning through Intra- and Inter-Annual Comparisons with Earth Observation Data. Remote Sens. 13, 3219.
- Petropoulos, G.P., Griffiths, H.M., Kalivas, D.P., 2014. Quantifying spatial and temporal vegetation recovery dynamics following a wildfire event in a mediterranean landscape using EO data and GIS. Appl. Geogr. 50, 120–131.
- Picotte, J.J., Robertson, K.M., 2011. Validation of remote sensing of burn severity in south-eastern US ecosystems. Int. J. Wildland Fire 20, 453–464.
- Poca, M., Cingolani, A.M., Gurvich, D.E., Saur Palmieri, V., Bertone, G., 2018. 2018. Water storage dynamics across different types of vegetated patches in rocky highlands of central Argentina (art. no). Ecohydrology 11 (7), e1981. https://doi.org/10.1002/eco.1981.
- Poon, P.K., Kinoshita, A.M., 2018. Spatial and temporal evapotranspiration trends after wildfire in semi-arid landscapes. J. Hydrol. 559, 71–83.
- Poulos, H.M., Barton, A.M., Koch, G.W., Kolb, T.E., Thode, A.E., 2021. Wildfire severity and vegetation recovery drive post-fire evapotranspiration in a southwestern pineoak forest, Arizona, USA. Remote Sens. Ecol. Conserv. 7 (4), 579–591. https://doi. org/10.1002/rse2.210.
- Probst, P., Boulesteix, A.L., 2018. To tune or not to tune the number of trees in Random Forest. J. Mach. Learn. Res. 18, 1–18.
- Quintano, C., Calvo, L., Fernández-Manso, A., Suárez-Seoane, S., Fernándes, P.M., Fernández-Guisuraga, J.M., 2023. First evaluation of fire severity retrieval from PRISMA hyperspectral data. Remote Sens. Environ. 295, 113670.

- Quintano, C., Fernández-Manso, A., Fernández-Manso, O., 2018. Combination of Landsat and Sentinel-2 MSI data for initial assessing of burn severity. Int. J. Appl. Earth Obs. Geoinf. 64, 221–224.
- Quintano, C., Fernández-Manso, A., Roberts, D.A., 2013. Multiple Endmember Spectral Mixture Analysis (MESMA) to map burn severity levels from Landsat images in Mediterranean countries. Remote Sens. Environ. 136, 76–88.
- Quintano, C., Fernández-Manso, A., Roberts, D.A., 2020. Enhanced burn severity estimation using fine resolution ET and MESMA fraction images with machine learning algorithm. Remote Sens. Environ. 244, 111815.
- Quintano, C., Fernández-Manso, A., Fernández-Guisuraga, J.M., Roberts, D.A., 2024. Improving fire severity analysis in mediterranean environments: a comparative study of eeMETRIC and SSEBop landsat-based evapotranspiration models (2024). Remote Sens. 16 (2), 361. https://doi.org/10.3390/rs16020361.
- Regos, A., Díaz-Raviña, M., 2023. A Storyboard of Wildfires in Galicia. In: Núñez-Delgado, A., Álvarez-Rodríguez, E., Fernández-Calviño, D. (Eds.), The Environment in Galicia: A Book of Images. Springer, Cham. https://doi.org/10.1007/978-3-031-33114-5 26.
- Rengers, F.K., McGuire, L.A., Oakley, N.S., Kean, J.W., Staley, D.M., Tang, H., 2020. Landslides after wildfire: initiation, magnitude, and mobility. Landslides 17, 2631–2641
- Rigge, M., Homer, C., Cleeves, L., Meyer, D.K., Bunde, B., Shi, H., Xian, G., Schell, S., Bobo, M., 2020. Quantifying Western U.S. Rangelands as Fractional Components with Multi-Resolution Remote Sensing and In Situ Data. Remote Sens. 12, 412.
- Riley, S.J., De Gloria, S.D., Elliot, R., 1999. Index that quantifies topographic heterogeneity Int. J. Sci. 5 (1999), 1–4.
- Rocha, A.V., Shaver, G.R., 2011. Postfire energy exchange in arctic tundra: the importance and climatic implications of burn severity. Glob. Chang. Biol 17, 2831–2841.
- Roche, J.W., Ma, Q., Rungee, J., Bales, R.C. 2020. Evapotranspiration Mapping for Forest Management in California's Sierra Nevada. Frontiers in Forests and Global Change, 3
- Sánchez, J.M., Bisquert, M., Rubio, E., Caselles, V., 2015. Impact of land cover change induced by a fire event on the surface energy fluxes derived from remote sensing. Remote Sens 7, 14899–14915.
- Savoca, M.E., Senay, G.B., Maupin, M.A., Kenny, J.F., Perry, C.A. 2013. Actual Evapotranspiration Modeling Using the Operational Simplified Surface Energy Balance (SSEBop) Approach; Scientific Investigations Report 2013–5126; U.S. Geological Survey: Reston, VA, USA.
- Seidl, R., Schelhaas, M., Rammer, W., Verkerk, P.J., 2014. Increasing forest disturbances in Europe and their impact on carbon storage. Nat. Clim. Change 4 (9), 806–810.
- Senay, G.B., 2018. Satellite psychrometric formulation of the operational simplified surface energy balance (SSEBop) model for quantifying and mapping evapotranspiration. Appl. Eng. Agric. 34, 555–566.
 Senay, G.B., Bohms, S., Singh, R.K., Gowda, P.H., Velpuri, N.M., Alemu, H., Verdin, J.P.,
- Senay, G.B., Bohms, S., Singh, R.K., Gowda, P.H., Velpuri, N.M., Alemu, H., Verdin, J.P., 2013. Operational evapotranspiration mapping using remote sensing and weather datasets: a new parameterization for the SSEB approach. J. Am. Water Resour. Assoc. 49 (3), 577–591.
- Senay, G.B., Budde, M.E., Verdin, J.P., 2011. Enhancing the Simplified Surface Energy Balance (SSEB) approach for estimating landscape ET: validation with the METRIC model. Agric. Water Manag 98, 606–618.
- Senay, G.B., Friedrichs, M., Morton, C., Parrish, G.E.L., Schauer, M., Khand, K., Kagone, S., Boiko, O., Huntington, J., 2022. Mapping actual evapotranspiration using Landsat for the conterminous United States: google earth engine implementation and assessment of the SSEBop model. Remote Sens. Environ. 275, 113011
- Senay, G.B., Kagone, S., Velpuri, N.M., 2020. Operational global actual evapotranspiration: development, evaluation, and dissemination. Sensors 20, 1915.
- Senay, G.B., Kagone, S. 2019. Daily SSEBop Evapotranspiration: U.S. Geological Survey Data Release; U.S. Geological Survey: Reston, VA, USA, 2019.
- Senay, G.B., Parrish, G.E.L., Schauer, M., Friedrichs, M., Khand, K., Boiko, O., Kagone, S., Dittmeier, R., Arab, S., Ji, L., 2023. Improving the operational simplified surface energy balance evapotranspiration model using the forcing and normalizing operation. Remote Sens 15, 260.
- Serrano-Notivoli, R., Tejedor, E., Sarricolea, P., Meseguer-Ruiz, O., de Luis, M., Saz, M. A., Longares, L.A., Olcina, J., 2023. Unprecedented warmth: a look at Spain's exceptional summer of 2022. Atmos. Res. 293, 106931. https://doi.org/10.1016/j.atmosres.2023.106931.
- Shrestha, S., Williams, C.A., Rogers, B.M., Rogan, J., Kulakowski, D., 2022. Wildfire controls on land surface properties in mixed conifer and ponderosa pine forests of Sierra Nevada and Klamath mountains, Western US (art. no). Agric. For. Meteorol. 320, 108939. https://doi.org/10.1016/j.agrformet.2022.108939.
- Singh, R.K., Senay, G.B., 2016. Comparison of four different energy balance models for estimating evapotranspiration in the Midwestern United States. Water $8\,1,\,9.$
- Singh, R.K., Senay, G.B., Velpuri, N.M., Bohms, S., Scott, R.L., Verdin, J.P., 2014. Actual evapotranspiration (Water Use) assessment of the Colorado River Basin at the landsat resolution using the operational simplified surface energy balance model. Remote Sens 6, 233–256.
- Speiser, J.L., Miller, M.E., Tooze, J., Ip, E., 2019. A comparison of random forest variable selection methods for classification prediction modeling. Expert Syst. Appl. 134, 93–101.
- Stephenson, N.L., 2003. Actual evapotranspiration and deficit: biologically meaningful correlates of vegetation distribution across spatial scales. J. Biogeogr. 25, 855–870.

- Su, Z., 2002. The Surface Energy Balance System (SEBS) for estimation of turbulent heat fluxes. Hydrol. Earth Syst. Sci. 6 (1), 85–100.
- Taulavuori, K., Laine, K., Taulavuori, E., 2013. Experimental studies on Vaccinium myrtillus and Vaccinium vitis-idaea in relation to air pollution and global change at northern high latitudes: a review. Environ. Exp. Bot. 87, 191–196. https://doi.org/10.1016/j.envexpbot.2012.10.002.
- Thornthwaite, C.W., 1948. An approach toward a rational classification of climate. Geogr. Rev. 38, 55–94.
- Turiel-Santos, S., Calvo, L., Martín Pinto, P., Taboada, A., 2024. Large wildfires alter the potential capacity of fire-prone Mediterranean pine forests to provide wild edible mushrooms over the long term (2024) Trees. For. People 18, 100658. https://doi.org/10.1016/j.tfp.2024.100658.
- Ueyama, M., Ichii, K., Iwata, H., Euskirchen, E.S., Zona, D., Rocha, A.V., Harazono, Y., Iwama, C., Nakai, T., Oechel, W.C., 2014. Change in surface energy balance in alaska due to fire and spring warming, based on upscaling eddy covariance measurements. J. Geophys. Res. Biogeosci. 119 (10), 1947–1969.
- Van der Tol, C., Norberto-Parodi, G., 2011. Guidelines for remote sensing of evapotranspiration. In: Irmak, A. (Ed.), In Evapotranspiration—Remote Sensing and Modeling. InTech: Rijeka, Croatia, pp. 227–250.
- Verhoef, W., Xiao, Q., Jia, L., Su, Z., 2007. Unified optical-thermal four-stream radiative transfer theory for homogeneous vegetation canopies. IEEE Trans. Geosci. Remote Sens. 45, 1808–1822.
- Viana-Soto, A., Aguado, I., Salas, J., García, M., 2020. Identifying post-fire recovery trajectories and driving factors using Landsat time series in fire-prone mediterranean pine forests. Remote Sens 12, 1499.
- Wasserman, T.N., Mueller, S.E., 2013. Climate influences on future fire severity: a synthesis of climate-fire interactions and impacts on fire regimes, high-severity fire, and forests in the western United States. Fire Ecol. 19 (43), 2023.
- White, D.A., Balocchi-Contreras, F., Silberstein, R.P., Ramírez de Arellano, P., 2020. The effect of wildfire on the structure and water balance of a high conservation value Hualo (Nothofagus glauca (Phil.) Krasser.) forest in central Chile. For. Ecol. Manag. 472
- Wilder, B.A., Kinoshita, A.M., 2022. Incorporating ECOSTRESS evapotranspiration in a paired catchment water balance analysis after the 2018 Holy Fire in California. Catena 215, 106300.
- Wine, M., Cadol, D., 2016. Hydrologic effects of large southwestern USA wildfires significantly increase regional water supply: fact or fiction? Environ. Res. Lett. 11, 085006.
- Xu, S., Qin, T., Lu, J., Liu, S., Hou, J., Feng, J., Li, W., Liu, H., Abebe, S.A., 2024. Identification of driving mechanisms of actual evapotranspiration in the Yiluo River Basin based on structural equation modeling. Ecol. Process 13 (69), 2024.
- Basin based on structural equation modeling. Ecol. Process 13 (69), 2024.
 Yao, Y., Liang, S., Cheng, J., Liu, S., Fisher, J.B., Zhang, X., Jia, K., Zhao, X., Qin, Q., Zhao, B., Han, S., Zhou, G., Zhou, G., Li, Y., Zhao, S., 2013. MODIS-driven estimation of terrestrial latent heat flux in China based on a modified Priestley–Taylor algorithm. Agric. For. Meteor. 171–172. 187–202.
- Yi, K., Senay, G.B., Fisher, J.B., Wang, L., Suvocarev, K., Chu, H., Moore, G.W., Novick, K. A., Barnes, M.L., Keenan, T.F., Mallick, K., Luo, X., Missik, J.E.C., Delwiche, K.B., Nelson, J.A., Good, S.P., Xiao, X., Kannenberg, S.A., Ahmadi, A., Wang, T., Bohrer, G., Litvak, M.E., Reed, D.E., Oishi, A.C., Torn, M.S., Baldocchi, D., 2024. Challenges and future directions in quantifying terrestrial evapotranspiration. Water Resour. Res. 60, e2024WR037622.
- Yin, L., Wang, X., Feng, X., Fu, B., Chen, Y., 2020. A comparison of SSEBop-model-based evapotranspiration with eight evapotranspiration products in the Yellow River Basin. China Remote Sens. 12, 2528.
- Yuan, W., Liu, S., Yu, G., Bonnefond, J.-M., Chen, J., Davis, K., Desai, A.R., Goldstein, A. H., Gianelle, D., Rossi, F., Suyker, A.E., Verma, S.B., 2010. Global estimates of evapotranspiration and gross primary production based on MODIS and global meteorology data. Remote Sens. Environ. 114, 1416–1431.
- Zahura, F., Bisht, G., Li, Z., McKnight, S., Chen, X., 2024. Impact of topography and climate on post-fire vegetation recovery across different burn severity and land cover types through random forest. Ecol. Inform. 82, 02757.
- Zalman, C., Hanna, E., Rush, J., Boise, K., Larios, L., 2023. Vegetation type and fire severity mediate short-term post fire soil microbial responses. Plant Soil 484, 155–170.
- Zhang, K., Kimball, J.S., Running, S.W., 2016. A review of remote sensing based actual evapotranspiration estimation. Wiley Interdiscip. Rev. Water 3 (6), 834–853.
- Zhang, X., Liu, M., 2022. Topography regulates the responses of water partitioning to climate and vegetation seasonality. Sci. Total Environ. 838, 156028 (art. no.).
- Zhao, J., Xu, Z.X., Singh, V.P., Zuo, D.P., Li, M., 2016. Sensitivity of potential evapotranspiration to climate and vegetation in a water-limited basin at the northern edge of Tibetan Plateau. Water Resour. Manag 30 (13), 4667–4680.
- Zhu, N., Wang, J., Luo, D., Wang, X., Shen, C., Wu, N., Zhang, N., Tian, B., Gai, A., 2024. Unveiling evapotranspiration patterns and energy balance in a subalpine forest of the Qinghai–Tibet Plateau: observations and analysis from an eddy covariance system. J. For. Res. 35, 53. https://doi.org/10.1007/s11676-024-01708-8.
- Zimba, H.M., Coenders-Gerrits, M., Banda, K.E., Hulsman, P., van de Giesen, N., Nyambe, I.A., Savenije, H.H.G., 2024. On the importance of plant phenology in the evaporative process of a semi-arid woodland: could it be why satellite-based evaporation estimates in the miombo differ? Hydrol. Earth Syst. Sci. 28 (15), 3633–3663.